EUROPEAN ORGANIZATION FOR NUCLEAR RESEARCH

CERN/ISRC/72-22
1 August 1972

PROPOSAL FOR AN EXPERIMENT ON THE MULTIGAMMA PRODUCTION AT THE CERN ISR

Luke C.L. Yuan, G.F. Dell and H. Uto,
Brookhaven National Laboratory,
Upton, New York, USA

E. Amaldi, M. Beneventano, B. Borgia and P. Pistilli,
Istituto di Fisica "Guglielmo Marconi",
Università degli Studi, Roma, Italy

John P. Dooher,
Grumman Aerospace Corporation,
Bethpage, New York, USA

Geneva - 1972

CONTENTS

1. INTRODUCTION

Some time ago we presented the proposal to search for high-energy multigamma events at the ISR and to study their characteristics and nature[1]. The experimental set-up designed in order to reach such a goal included a series of hodoscope lead-glass Čerenkov counters sandwiched with a number of proportional wire chambers.

The ISR Committee recognized the interest of the physical problem, but, in order to avoid the preparation of a new expensive set-up, suggested that an exploratory search for multigamma events could be started by making use of equipment already installed at the ISR for some other experiment.

Since it was clear from the beginning that the type of device necessary for our research was in some way similar to that constructed by the CERN-Columbia-Rockfeller Group (CCR Group) we got in touch with the members of this group, who were extremely kind and helpful in trying to find a solution which could satisfy us without interfering with their own experiment.

The arrangement agreed upon with the CCR group is based on the idea that we can share the use of their scintillation counters, lead-glass counters, and spark chambers, and even of their recording system, by interposing different logics. In this way the two experiments can be run at the same time.

This solution has many advantages; in particular, it reduces the cost and time of preparation of the experiment. It has, however, the disadvantage that the solid angle covered by the CCR detection system is only 20% of the total, while the set-up of our original proposal covered more than 60%.

The solution adopted for reaching the goal of the "contemporary double use" of the same detection system is based on the insertion, at convenient points of the circuits of the CCR Group, of a number of "fan-out" units which split the pulses into identical multiple outputs which can then be shared by our two groups.

The multiple events in which we are interested are triggered by our electronics and logic system; this trigger is fed into the master trigger system for their computer, and our desired events are registered and recorded on the same magnetic tape.

Data were collected regularly with such an equipment-sharing arrangement, whenever the ISR were operated for physics, during the last few months of 1971 and the first part of 1972. Some preliminary results from this exploratory experiment are presented in Section 3 of the present proposal, while Section 2 contains a summary of the physical considerations, which, in the opinion of the proponents, justify a considerable effort in this direction. These are discussed in more detail in Appendix A.

Section 4 contains a proposal for a simple method of increasing the solid angle by the addition of some multiwire proportional chambers (MWPC) which will not interfere in any way with the work of the CCR Group. In view of such a possible extension of the experiment, a prototype multiwire proportional chamber was constructed at CERN during the winter of 1971, and it has been extensively tested with radioactive sources and in a 6.4 GeV/c π^- beam of the PS. The results of these tests are presented in Section 5, and details of the MWPC are given in Appendix C.

2. SOME ASPECTS OF PHYSICAL INTEREST

Our interest in this type of research is motivated by various considerations. The first one is the observation by various authors[2-4] of multigamma-ray events in stacks of nuclear emulsions exposed to cosmic rays at high altitude. These events could not be accounted for either by conventional electromagnetic showers originating from a single high-energy gamma (or electron), or by conventional nuclear interaction in the production of many π^0's. Rather, they appear to be a result of a large number of gammas produced simultaneously in a single process. These events are discussed below in more detail (Section 2.1). They remained a mystery for a number of years, until rather recently Ruderman and Zwanziger[5] put forward a plausible explanation. They could be due to the creation and subsequent annihilation of Dirac magnetic monopole pairs. This assumption was discussed in detail in our previous Revised Proposal, CERN/ISRC/70-19/Rev 2. The main points discussed there are summarized in Section 2.2.

Two other processes have been considered as possible explanations of the cosmic-ray events mentioned above[1c]. The first one, suggested by

T.D. Lee, consists in the production and immediate annihilation of a pair of leptons of high Z. This process is very similar to that proposed by Ruderman and Zwanziger with the possibility that it is characterized by different energy and angular distributions.

A third process, suggested independently by Winter[6] and Lee[1c], consists in the production of a heavy boson of high total angular momentum J. For sufficiently large values of J and mass M_J the dominating decay process of this particle would consist in the emission of a series of photons of energy $h\nu < m_\pi c^2$. For a more detailed discussion of this process, we refer to the paper by Winter[6].

The present proposal is primarily an extension of the current exploratory experiment aimed at achieving a much more meaningful investigation of the existence and frequency of multigamma-ray events, the interpretation of which can either lead to the necessity for some more specific experiments to be made at a later time, or to the recognition of some revealing features of the observed events.

From the experimental point of view, the main problem involved in the establishment of the existence of multigamma events consists in distinguishing them from the background of gamma-rays produced in the decay of many neutral pions (and other secondary particles) produced in p-p collisions at the ISR energy.

The study of the last process, however, is exceedingly interesting in itself, and would provide information of tremendous value on the multiple production of hadrons.

This point will be discussed in more detail in Section 2.3, where it will be shown that an experiment of the type proposed here is valuable and worth doing even if multigamma-ray events were not observed, or were observed only as extreme fluctuations of the multiple production of neutral pions.

3. PRELIMINARY RESULTS OF THE EXPLORATORY EXPERIMENT OBTAINED WITH THE SHARING OF THE DETECTION SYSTEM OF THE CCR GROUP

In the early phase of our exploratory experiment on the search for multigamma-rays at the ISR, some very preliminary results[1e] were reported to the ISR Committee when only one side of the full two-sided

detection system of the CCR experiment was set up. Since April of this year, the complete detection system of the CCR Group has been set up and is in operation; our electronics and logic system was also doubled and greatly improved in the course of fully sharing the CCR complete detection system. We are deeply indebted to the various members of the CCR Group who have helped us without reservation to accomplish the successful sharing of the use of their detectors, as well as with data recording. In the meantime we have also augmented our electronics and logic system by purchasing an HP2100A computer and magnetic tape recorder, 48 channels of specially designed ADC units (analogue-to-digital converter), a Camac manual controller, and an all-Camac system for on-line operation for monitoring and recording certain specific data that are of particular interest.

Extracting our triggered events from the magnetic tape used jointly with the CCR Group, we have succeeded in writing a computer program (global program) for analysing some of our desired results mainly from the data recorded by the 32 lead-glass slabs called HV counters (14.6 cm × 35 cm in area and 7.2 cm in thickness), 120 large lead-glass blocks called LB counters (14.6 cm × 14.6 cm in area and 35 cm long), and 20 scintillation counters called Z counters which were added since April by the CCR Group to further reduce their background and to increase their trigger requirements. These Z counters (50 × 6.5 cm in size and placed vertically 10 in a row on each side of the interaction region) also help us in obtaining some information on the extent of charged particles accompanying our multigamma events. Very recently the CCR Group has also very kindly made available to us their computer program on the track fitting of the spark chamber data of the charged particles. We are in the process of writing a similar program to extract the charged particle events that are correlated to our triggered multigamma events. Such information would further help us in isolating any possible non-π^0 events, should they exist; and give some idea of the ratio of uncharged to charged particle production (of course within the 20% solid angle region around 90°), etc.

We shall present here some of the preliminary results which we have analysed. For convenience we shall designate the firing of any single HV counter as a single event. Since the threshold energy for triggering of any HV counter is set at 160 MeV, which is much higher than the energy loss of a high-energy charged particle coming from the general direction

of the interaction region, we could label each triggered HV event as a gamma-ray. However, the exact energy of this triggered HV event, as well as those of all the other HV events which are fired simultaneously, will be measured and recorded on the magnetic tape. So the energy of each individual event can be checked. It should be noted that as the area presented by the HV blocks to the interaction is quite large (7.2 × 35 cm), a triggered HV event could be the result of one or more simultaneous events. Hence the multiplicities of the measured γ's could be the lower limit of the real multiplicities. For the first part of the preliminary results presented here, we had to have at least four HV counters triggered simultaneously, i.e. corresponding to four or more multigamma events, and the beam energies for these data are 25 GeV in each beam. The triggered signals were always in coincidence with an interaction event registered in the beam-beam counter (R_1R_2), and the noise pick-ups such as beam spikes, spark chamber discharges, etc., were all eliminated by veto signals. The background in these results was measured by using a single beam only, and it is subtracted out after normalization. By using a rather crude but straightforward normalization method, the background amounted to a few per cent of the measured events.

The data presented below (Figs. 1 to 7) are taken under the condition that a lead-plate converter of 1 radiation length thick is placed immediately in front of the Z counters on the side facing the interaction region. This condition applies to both sides of the interaction region. Also, the triggers for these data are $\geq$ 4 HV's. Some representative data with no lead converter but with the triggers $\geq$ 3 HV's will also be shown (Figs. 8 and 9).

Figure 1 shows the number of HV and Z counters firing per triggered event (i.e. $\geq$ 4 HV's firing simultaneously). We see that the most preponderant number of HV counters firing is eight, among a total number of 32, although as many as 17 HV's are firing on five occasions in this run. Although we have taken all the usual precautions, our main concern is still to make sure that the firing of all these HV's is due only to gamma-rays. Should this be true, then the multiplicity within a comparatively small solid angle (20% of the total solid angle) is already much higher than one would expect in the usual production process, and the extension of these measurements to cover a much larger solid angle would be extremely

important. The most preponderant number of Z counters firing per triggered event also happens to be eight. However, the size of a Z counter is larger than that of an HV counter such that each Z counter covers about two HV's, and a meaningful correlation between these two can only be obtained when the spark chamber data are analysed for each individual event.

Figure 2 shows the energy distribution of a single HV counter (data for all the HV's, i.e. both the inside and outside HV's, are combined). It seems to indicate that most of the HV's firing in excess of the four triggered HV's (threshold energy = 160 MeV) are of the order of 40 MeV. These could be either low-energy gamma-rays or charged particles. It is interesting to note that there is a knee in the energy distribution curve at around 200 MeV. The highest energy in a single HV counter in this case is $\sim$ 640 MeV.

The total energy distribution (LB + HV inside and outside) is shown in Fig. 3. It is seen that the preponderant total energy per triggered event is $\sim$ 2 GeV with a maximum total energy of $\sim$ 6 GeV.

The energy distribution per triggered event in the HV's (inside and outside, respectively) is shown in Fig. 4, and a similar energy distribution for the (LB + HV)'s (inside and outside) is shown in Fig. 5. The distribution of energy in all HV's and in all LB's is shown in Fig. 6. The energy distribution of a single LB counter (inside or outside) is shown in Fig. 7. Owing to the centre-of-mass angle of the two colliding beams, there is a preponderance of higher energy events in the outside region, as indicated by the above-mentioned curves.

With the lead converter removed from in front of the Z counters, we have recently analysed the data from a run at the same beam energies (26 GeV/26 GeV) but with a less stringent trigger of $\geq$ 3 HV's. Figure 8 (solid curve) shows the total energy $\left[\Sigma(\text{HV} + \text{LB})\right]$ distribution per triggered event of $\geq$ 3 HV's, whereas the dotted curve shows the background in a scale which is larger by a factor of 10. Here the background is about 3%. For the more stringent triggers of $\geq$ 4 HV's the background would be even smaller. Figure 9 shows the energy distribution of a single HV counter also with a trigger of $\geq$ 3 HV's, and this curve also exhibits a knee similar to the one seen with the lead converter in place.

The data given above are obtained from the data of four typical runs out of ten analysed so far. At the end of July the total number of successful runs was about 100. The analysis was made by means of what we call our global program, which does not make use of the information from the spark chambers. A detailed analysis of each event, with a complete program, will be made as soon as possible.

4. PROPOSAL FOR A SIMPLE METHOD OF INCREASING THE SOLID ANGLE OF THE DETECTOR SYSTEM FOR THE DETECTION OF MULTIGAMMA-RAYS

We propose to add a system of large area MWPC arranged in sandwich pairs with a lead-plate converter in between each pair. The first wire chamber detects the number of charged particles and the second chamber behind the converter detects the number of gamma-rays. These chambers are of 1 m^2 in effective area, and each chamber consists of two signal wire planes perpendicular to each other. We plan to place four sandwich-pairs of these chamber systems (a total of eight individual chambers) in the neighbourhood of the forward and backward regions so that they can be located as close as possible to the interaction region without interfering with the CCR detection system (see Figs. 10 and 11; however, Fig. 11 only represents one half of the set-up). As a later step we also propose to place a simple scintillation counter or flash-tube hodoscope array in a lead-sandwich fashion both on top of and below the interaction on region to further increase the solid angle. In the first step we propose to place only two wire chamber pairs, which we hope to have ready by early November and certainly not later than late November if our proposal is approved. In the second step, at a later time, we hope to put in the other two pairs of chambers and, if possible, the simple scintillation counter or flash-tube hodoscopes on top of and below the interaction region.

We have consulted the CCR Group about the proposed addition of wire chambers, and they agreed to our proposal as long as these chambers will be placed in such a position that they will not interfere with their measurements.

We hope that it will be possible to place the wire chambers in close proximity to the interaction region so as to increase appreciably the solid angle covered by the combined gamma-ray detectors. However, even in the

case that this will not be feasible (without interfering with the CCR experiment), the fact of being able to measure, in each triggered event, the secondaries emitted in the direction close to the beam directions as well as those emitted around 90° will certainly be of the utmost importance.

5. DETAILS OF THE TESTS ON WIRE GROUPING IN A MULTIWIRE PROPORTIONAL CHAMBER

In order to obtain high detection efficiency and ease of operation, a wire chamber with an effective area of 1 m^2 and a wire spacing of 3 mm was constructed. Since the resolution in the space location of the multi-gamma events does not need to be high in an inherent centre-of-mass system which is characteristic of a colliding beam machine, much economy can be realized if a number of signal wires can be grouped together, which reduces the number of amplifier + logic channels by a factor equivalent to the number of wires grouped together. Otherwise one such channel would be required by each individual wire. It was decided that an eight-wire grouping would be a good compromise in space resolution and an economy in the electronics systems' cost. Although a seven-wire grouping in a smaller size (50 cm × 50 cm) wire proportional chamber has been successfully used (with 5 mm spacing and a standard argon-methane gas mixture) at Brookhaven on another experiment[7], and similar wire groupings have also been tried[8] in comparatively small chambers, no data seem to be available on eight-wire grouping in large chambers such as those having a 1 m^2 effective area. A grouping together of such long wires would certainly present a considerably higher effective input capacity, thus reducing appreciably the chamber signal pulse-height. The main purpose of the present investigation on the wire grouping effect is to ascertain to what extent an eight-wire grouping in such a large-size chamber will affect the signal output; and what kind of simple and economic preamplifier with a sufficient gain to give an adequately safe signal-to-noise ratio, and to yield a 100% detection efficiency in the chambers, will be required.

A prototype multiwire proportional chamber was designed, constructed, and kindly provided by the CERN NP Division so that we could make a thorough investigation of this matter.

This chamber consists of one signal wire plane, with a wire spacing of 3 mm, and two high-voltage wire planes of 1 mm wire spacing on either side of the signal wire plane. Tests were performed on this chamber using radioactive sources and in a 6.4 GeV/c π^- beam. Different gas mixtures and two different types of preamplifiers were also tried. A detailed description of these tests and the results obtained are contained in Appendix C.

Using a high-gain current amplifier specially designed[9] by the NP Electronics Group, and using the "magic gas" mixture in the chamber, a good high-voltage plateau curve was obtained (as shown in Fig. 12) with a 100% detection efficiency at 4 kV operating voltage. The chamber noise and noise pick-up problems at the PS have also been carefully investigated; these are also described in detail in Appendix C.

The main conclusions of these tests are that

a) the detection efficiency of the wire chamber filled with the "magic gas" and using a high-gain current amplifier is 100% at 4 kV;

b) the effects of the chamber noise and all other noise pick-ups can easily be eliminated;

c) the present design of the wire chamber as demonstrated by the tests performed with the prototype chamber has shown that it operates extremely well and remains stable over long periods of time.

We are deeply indebted to Prof. G. Charpak for many helpful suggestions and valuable discussions, and we are grateful to Dr. G. Muratori, Messrs. F. Doughty and J. Guezennec for the design and construction of the prototype wire chamber, and to Messrs. H. Verweij and J. Tarlé for the design and construction of the preamplifiers and helpful discussions. We also wish to express our grateful thanks to the Rome-Rutherford Group for letting us install our chamber and counter telescope in their pion beam, and for their generous help in many ways.

REFERENCES

1) L.C.L. Yuan, G.F. Dell and H. Uto; E. Amaldi, M. Beneventano, B. Borgia and P. Pistilli; and J.P. Dooher:
a) CERN/ISRC/70-19, October 2, 1970
b) CERN/ISRC/70-19 Rev. 1, November 1970
c) CERN/ISRC/70-19 Rev. 2, Spring 1971
d) CERN/ISRC/70-19/Add. 1, 27 May 1971
e) CERN/ISRC/70-19/Add. 2, 7 February 1972.

2) M. Schein, D.M. Haskin and M.G. Glasser, Phys. Rev. 95, 855 (1954); 99, 643 (1955).

3) A. Debenedetti, C.M. Garelli, L. Tallone and M. Vigone, Nuovo Cimento 2, 220 (1955); 4, 1151 (1956).
A. Debenedetti, C.M. Garelli, L. Tallone, M. Vigone and G. Wataghin, Nuovo Cimento 3, 226 (1956).

4) A. Jurak, M. Miesowicz, O. Stanisz and W. Wolter, Bull. Acad. Pol. Sci. Cl. III, 3, 369 (1955).
M. Koshiba and M.F. Kaplon, Phys. Rev. 100, 327 (1955).
L. Barbanti-Silva, C. Bonacini, C. De Pietri, I. Iori, G. Lovera, R. Perilli-Fedeli and A. Roveri, Nuovo Cimento 3, 1465 (1956).

5) M.A. Ruderman and D. Zwanziger, Phys. Rev. Letters 22, 146 (1969).

6) G. Neuhofer, F. Niebergall, J. Penzias, M. Regler, K.R. Schubert, P.E. Schumacher, W. Schmidt-Parzefall and K. Winter, Phys. Letters 37 B, 438 (1971).
G. Neuhofer, F. Niebergall, J. Penzias, M. Regler, W. Schmidt-Parzefall, K. Schubert and K. Winter, CERN/ISRC/70-18, 29 September 1970.

7) L.C.L. Yuan, H. Uto, G.F. Dell Jr. and P.W. Alley, to be published in Physics Letters.

8) R. Bouclier, G. Charpak, Z. Dimčovski, G. Fischer and F. Sauli, Nuclear Instrum. Methods 88, 149 (1970).

9) J. Lindsay, J. Tarlé, H. Verweij and H. Wendler, to be published.

* * *

The following references are called in the Appendices:

10) J.L. Neumeyer and J.S. Trefil, Phys. Rev. Letters 26, 1509 (1971).

11) B. Borgia, F. Ceradini, M. Conversi, L. Paoluzzi and R. Santonico, Nuovo Cimento Letters 3, 115 (1972).

12) J.H. Christienson, G.S. Hicks, L.M. Lederman, P.J. Limon, B.G. Pope and E. Zavattini, Phys. Rev. Letters 25, 1523 (1970).

13) In Ref. 1c we used the formula by G. Altarelli, R.A. Brandt and G. Preparata, Phys. Rev. Letters 26, 42 (1971), which is rather optimistic, as one can recognize from the comparison with other theoretical estimates shown in Fig. 2 of L.M. Lederman and B.G. Pope, Phys. Rev. Letters 27, 765 (1971).

14) R.A. Brandt and G. Preparata, BNL 16183, September 1971.

15) L.M. Lederman, Memo of the Columbia University, Spring 1972.

16) K.G. Wilson, Lab. of Nuclear Studies, Cornell Univ. Report CLNS-131, November 1970.

17) L. Van Hove, Phys. Letters 1 C, 347 (1971).

18) A.N. Diddens and K. Schlüpmann, Handbuch der Physiks, 1971 (Springer-Verlag, 1971).

19) J.C. Sens, 4th Int. Conf. on High-Energy Collisions, Oxford (1972).

20) O. Czyzewski and K. Rybicki, 15th Int. Conf. on High-Energy Physics, Kiev (1970).

21) C.P. Wang, Nuovo Cimento 64, 546 (1969); Phys. Letters 30 B, 115 (1969); Phys. Rev. 180, 1463 (1969).

22) C.P. Wang and A.L.L. Lin, Phys. Letters 35 B, 424 (1971), and Cavendish Lab. Preprint HEP 71-9.

23) G.F. Chew and A. Pignotti, Phys. Rev. 176, 1212 (1968).

24) A. Ballestrero, A. Giovannini, R. Nulman and E. Predazzi, Nuovo Cimento 5 A, 197 (1971).

25) W. Furry, Phys. Rev. 52, 569 (1937).

26) C. Quigg, Jiunn-Ming Wang and Chen Ning Yang, Phys. Rev. Letters 28, 1290 (1972).

Figure captions

Fig. 1 : Number of HV and number of Z counters firing per triggered event ($\geq$ 4 HV's). E = 26.7 GeV. Pb converter in place.

Fig. 2 : Distribution of energy deposited in a single HV counter. Trigger $\geq$ 4 HV's. E = 26.7 GeV. Pb converter in place.

Fig. 3 : Distribution of energy deposited in all the lead-glass counters (HV + LB). Trigger $\geq$ 4 HV's. E = 26.7 GeV. Pb converter in place.

Fig. 4 : Distribution of energy deposited in the HV counters. Trigger $\geq$ 4 HV's. E = 26.7 GeV. Pb converter in place.

Fig. 5 : Distribution of energy deposited in each side of the detector. Trigger $\geq$ 4 HV's. E = 26.7 GeV. Pb converter in place.

Fig. 6 : Comparison of the energy deposited in all HV counters with the energy deposited in all LB counters. Trigger $\geq$ 4 HV's. E = 26.7 GeV. Pb converter in place.

Fig. 7 : Distribution of energy deposited in a single LB counter. Trigger $\geq$ 4 HV's. E = 26.7 GeV. Pb converter in place.

Fig. 8 : Distribution of the energy deposited in all the lead-glass counters for a single beam and for two beams. Trigger $\geq$ 3 HV's. E = 26.6 GeV. No Pb converter.

Fig. 9 : Distribution of energy deposited in a single HV counter. Trigger $\geq$ 3 HV's. 26.6 GeV. No Pb converter.

Fig. 10 : Proposed placement of additional wire chambers and scintillation counters.

Fig. 11 : Plan of one side of the CCR detector system.

Fig. 12 : Voltage plateau of the 1 m^2 test chamber when filled with magic gas.

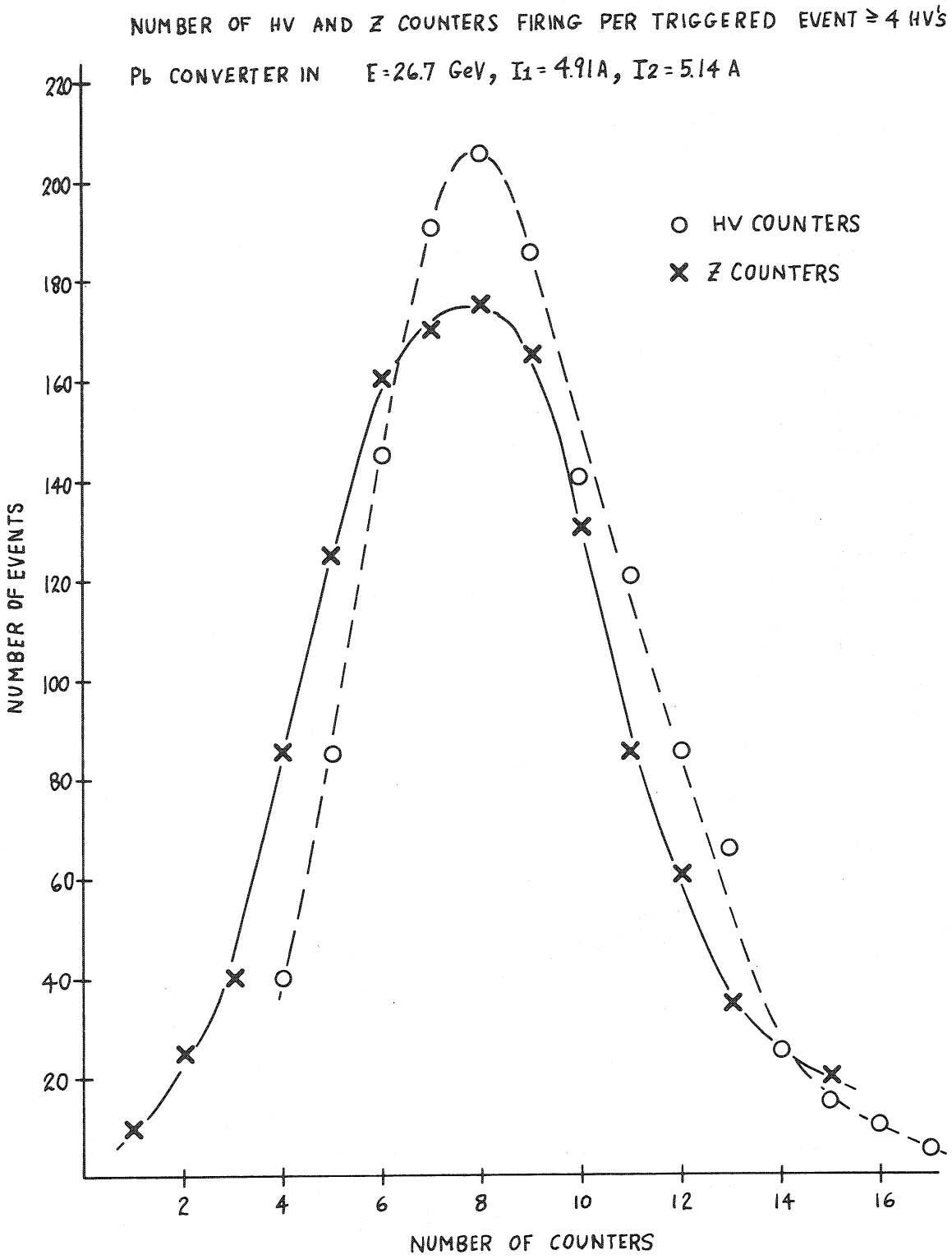
NUMBER OF HV AND Z COUNTERS FIRING PER TRIGGERED EVENT ≥ 4 HV's
Pb CONVERTER IN E=26.7 GeV, I1 = 4.91A, I2 = 5.14 A
HV COUNTERS
Z COUNTERS
NUMBER OF EVENTS
NUMBER OF COUNTERS
220
200
180
160
140
120
100
80
60
40
20
2
4
6
8
10
12
14
16

Fig. 1

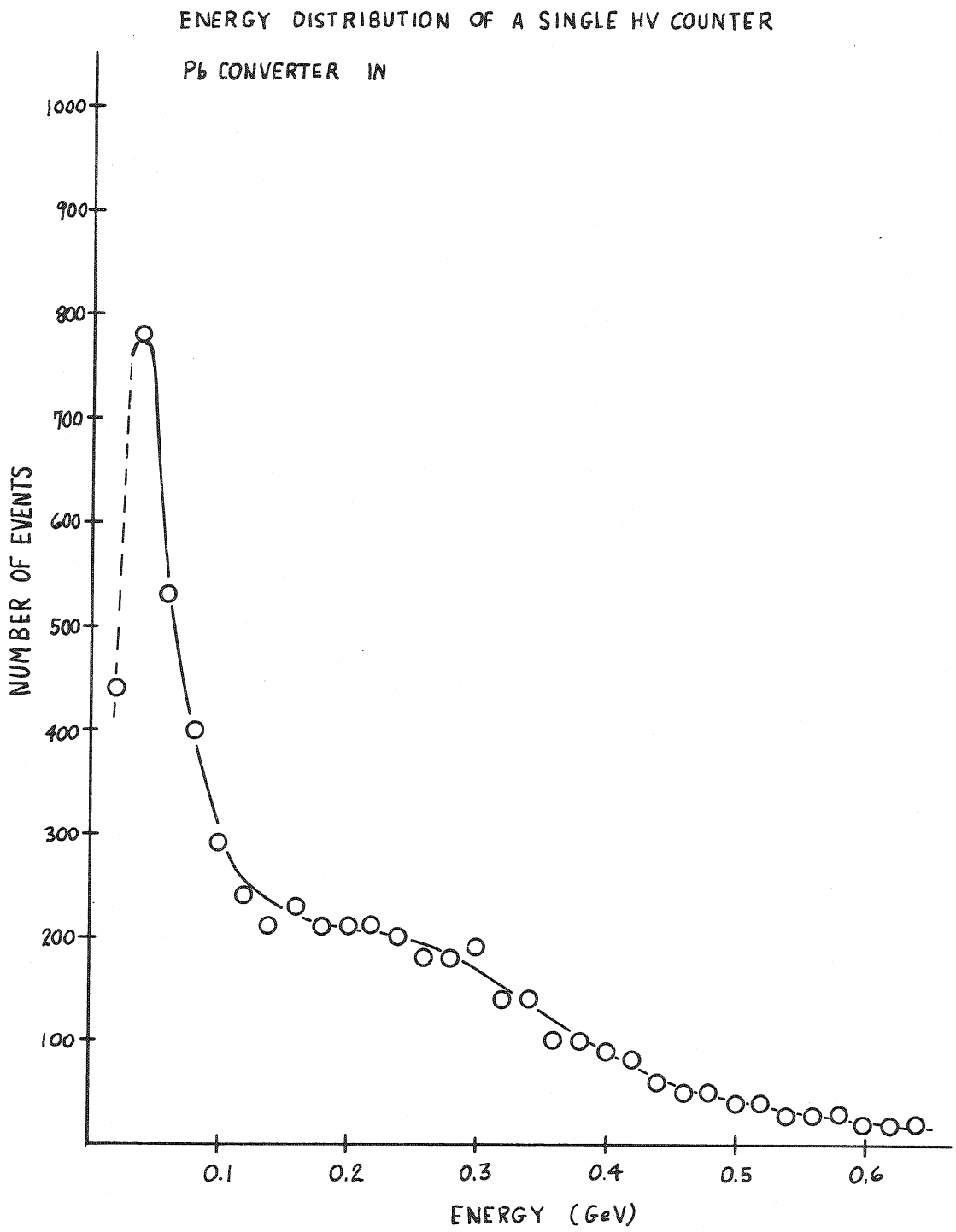
ENERGY DISTRIBUTION OF A SINGLE HV COUNTER
Pb CONVERTER IN
NUMBER OF EVENTS
1000
900
800
700
600
500
400
300
200
100
0.1
0.2
0.3
0.4
0.5
0.6
ENERGY (GeV)

Fig. 2

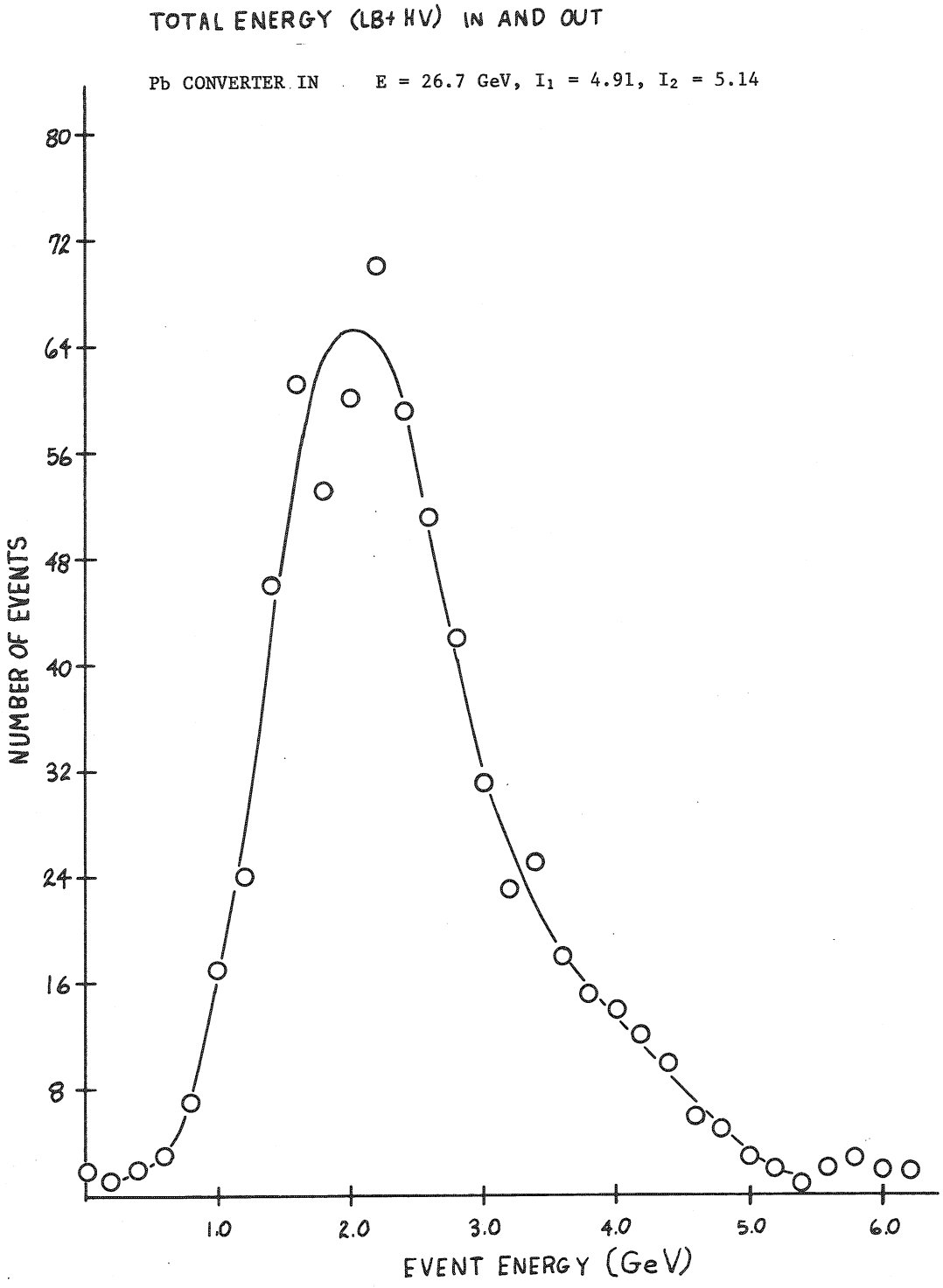
TOTAL ENERGY (LB+HV) IN AND OUT
Pb CONVERTER IN
E = 26.7 GeV, I_1 = 4.91, I_2 = 5.14
NUMBER OF EVENTS
80
72
64
56
48
40
32
24
16
8
1.0
2.0
3.0
4.0
5.0
6.0
EVENT ENERGY (GeV)

Fig. 3

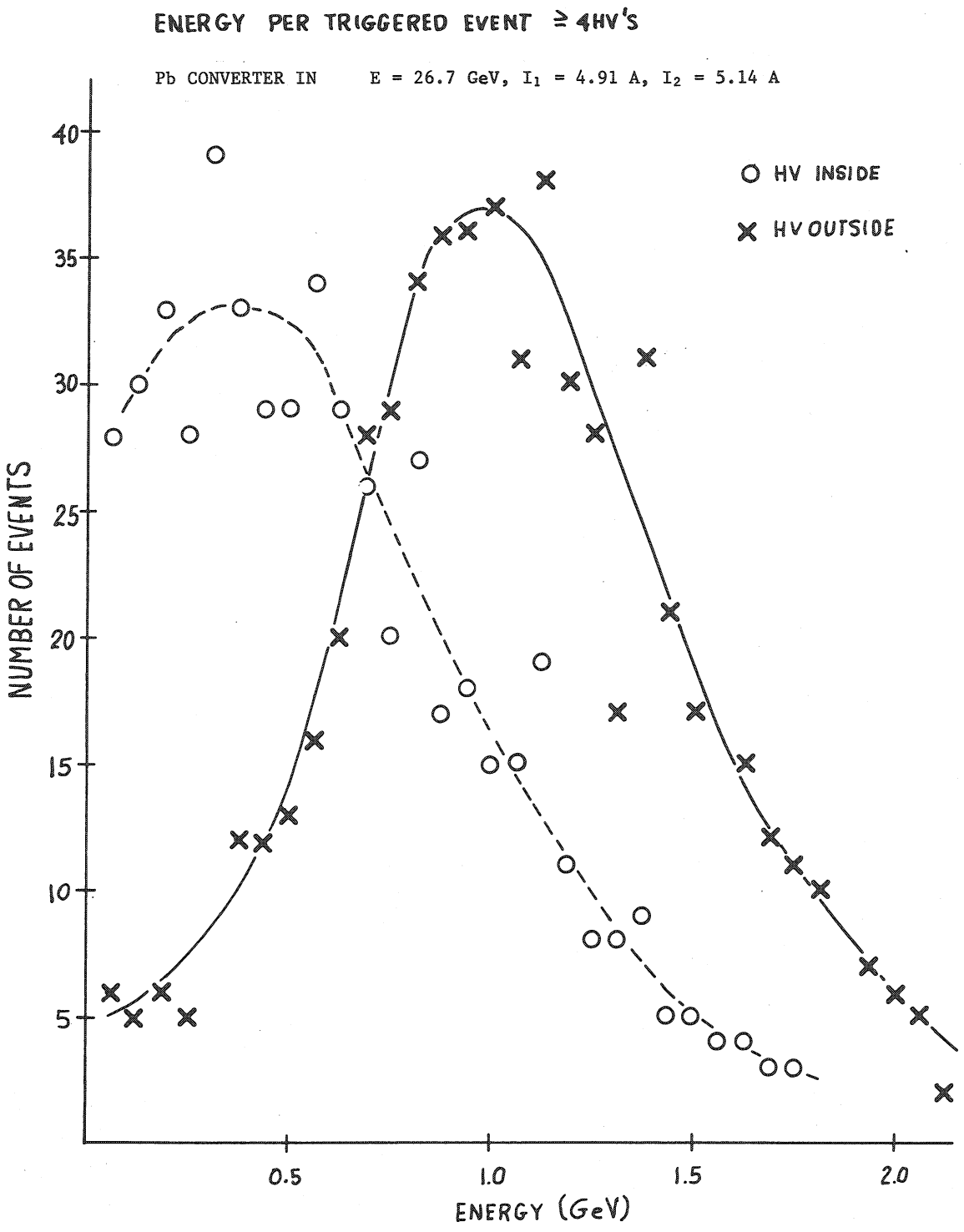
ENERGY PER TRIGGERED EVENT ≥ 4HV'S
Pb CONVERTER IN
E = 26.7 GeV, I_1 = 4.91 A, I_2 = 5.14 A
HV INSIDE
HV OUTSIDE
NUMBER OF EVENTS
ENERGY (GeV)
40
35
30
25
20
15
10
5
0.5
1.0
1.5
2.0

Fig. 4

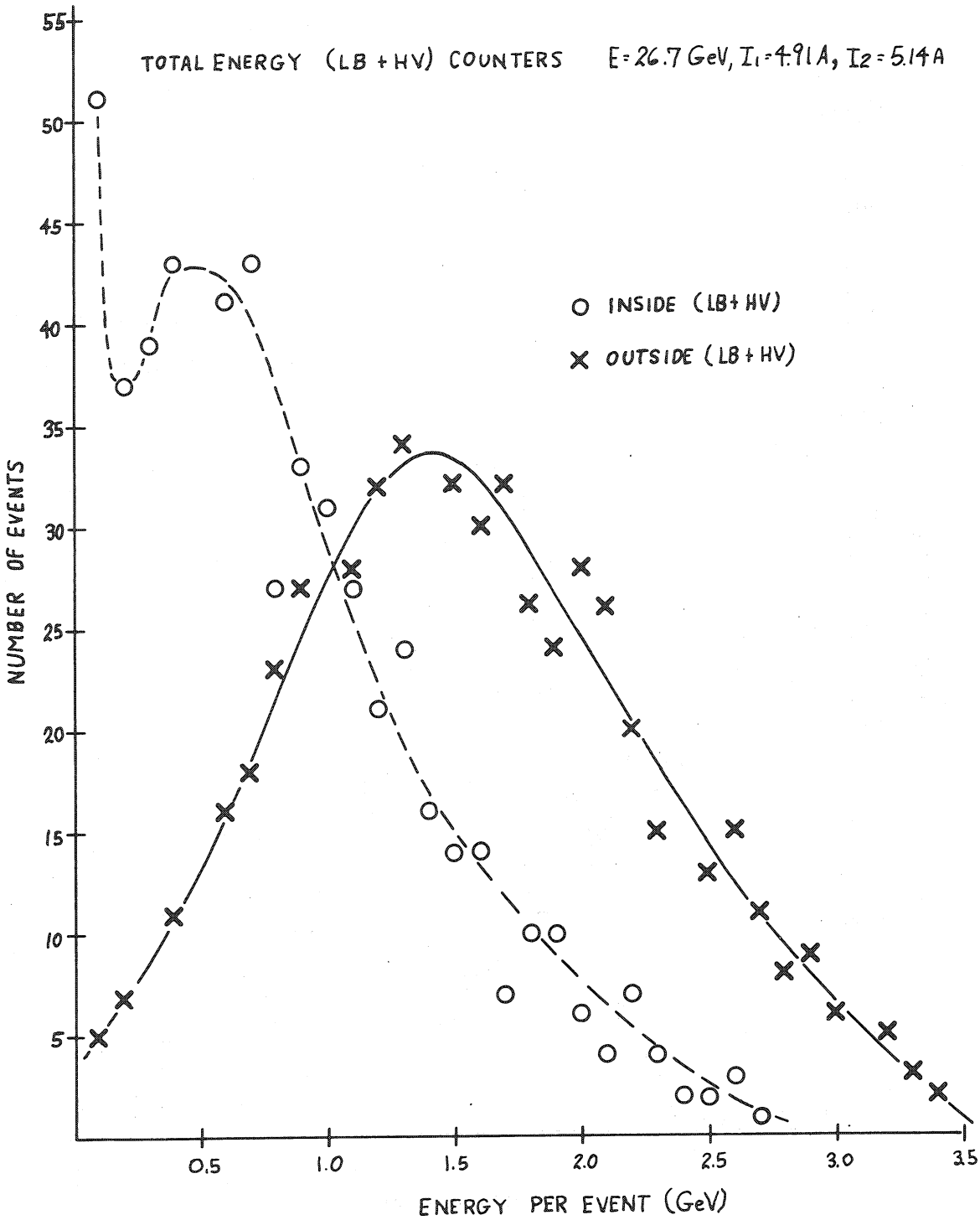
TOTAL ENERGY (LB + HV) COUNTERS E=26.7 GeV, I1=4.91A, I2=5.14A
O INSIDE (LB+HV)
× OUTSIDE (LB+HV)
NUMBER OF EVENTS
ENERGY PER EVENT (GeV)
55
50
45
40
35
30
25
20
15
10
5
0.5
1.0
1.5
2.0
2.5
3.0
3.5

Fig. 5

DISTRIBUTION OF ENERGY DEPOSITED IN ALL HV'S AND IN ALL LB'S

Pb CONVERTER IN E = 26.7 GeV, I_1 = 4.91 A, I_2 = 5.14 A

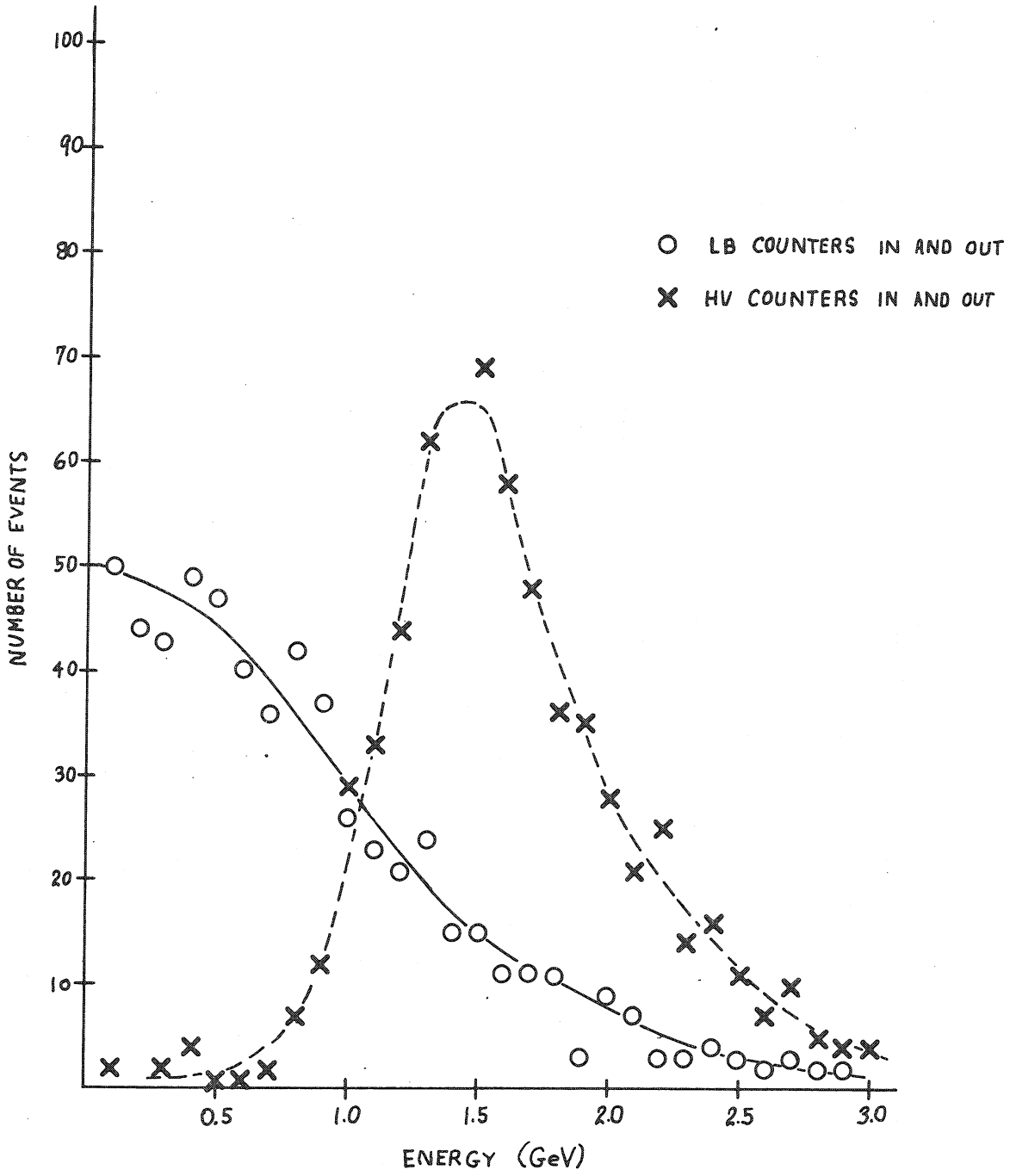

Fig. 6

ENERGY DISTRIBUTION OF A SINGLE LB COUNTER

Pb CONVERTER IN E = 26.7 GeV, I_1 = 4.91 A, I_2 = 5.14 A

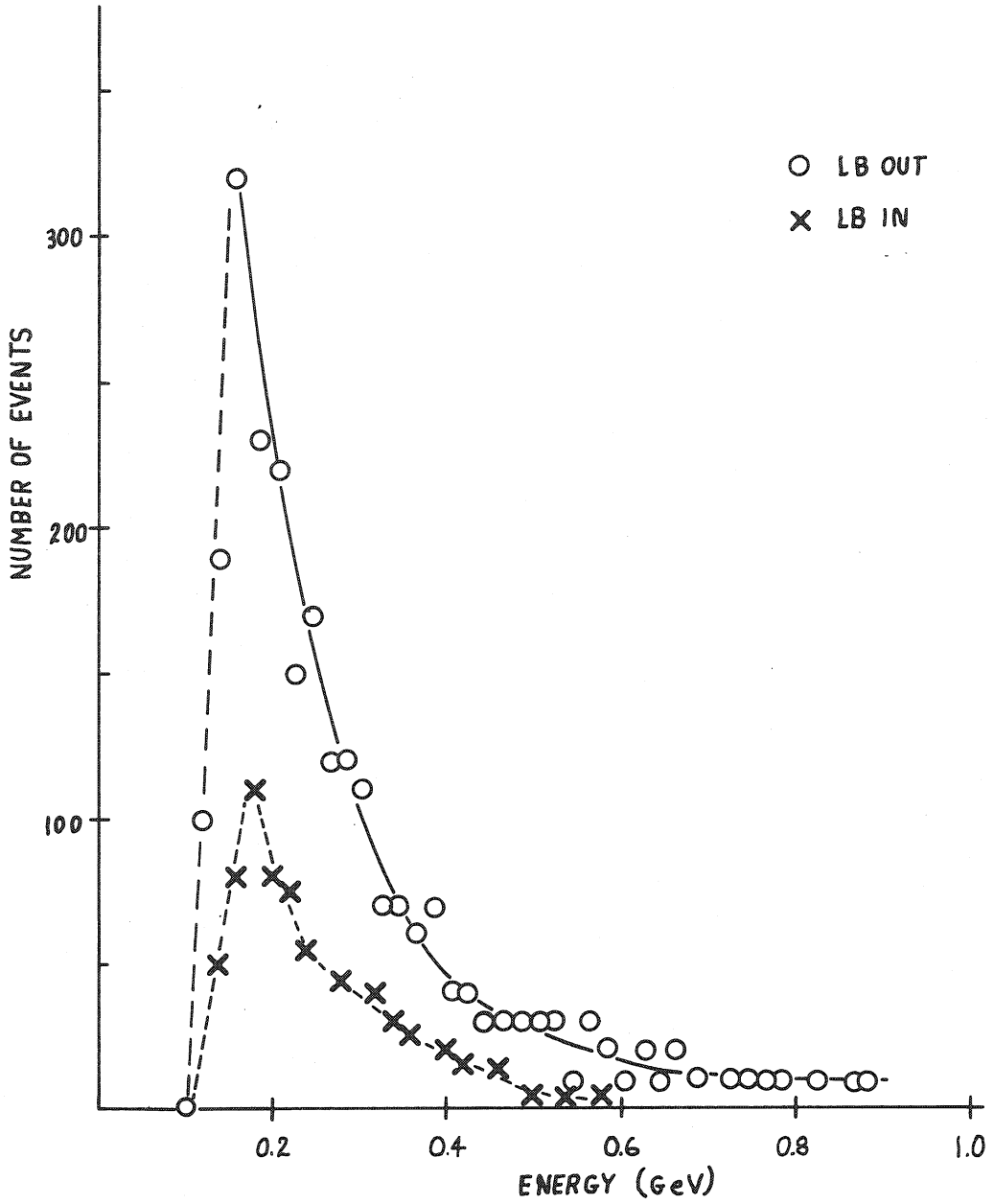

Fig. 7

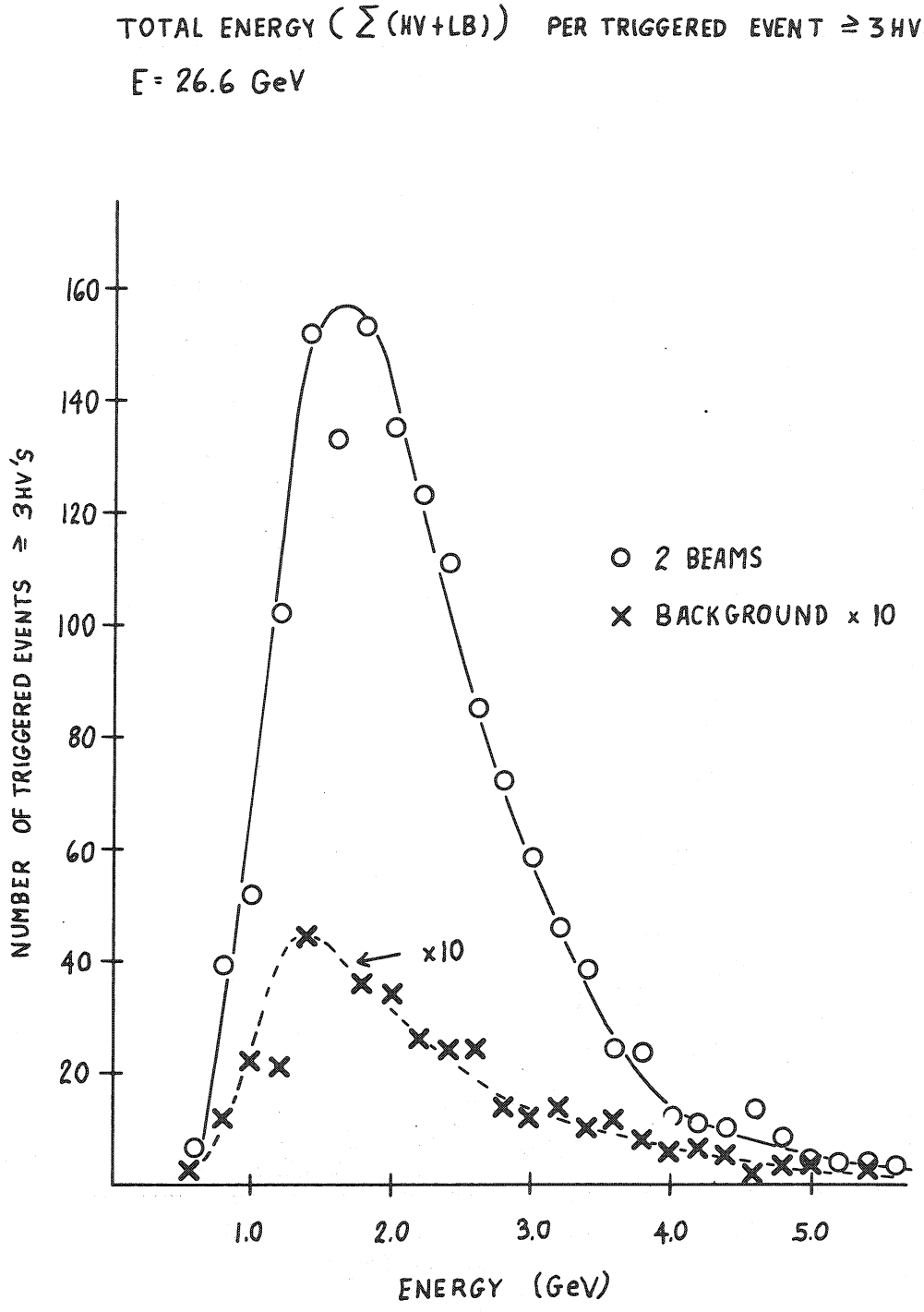
TOTAL ENERGY (Σ (HV+LB)) PER TRIGGERED EVENT ≥ 3 HV's
E = 26.6 GeV
NUMBER OF TRIGGERED EVENTS ≥ 3 HV's
160
140
120
100
80
60
40
20
1.0
2.0
3.0
4.0
5.0
ENERGY (GeV)
2 BEAMS
BACKGROUND x 10
x10

Fig. 8

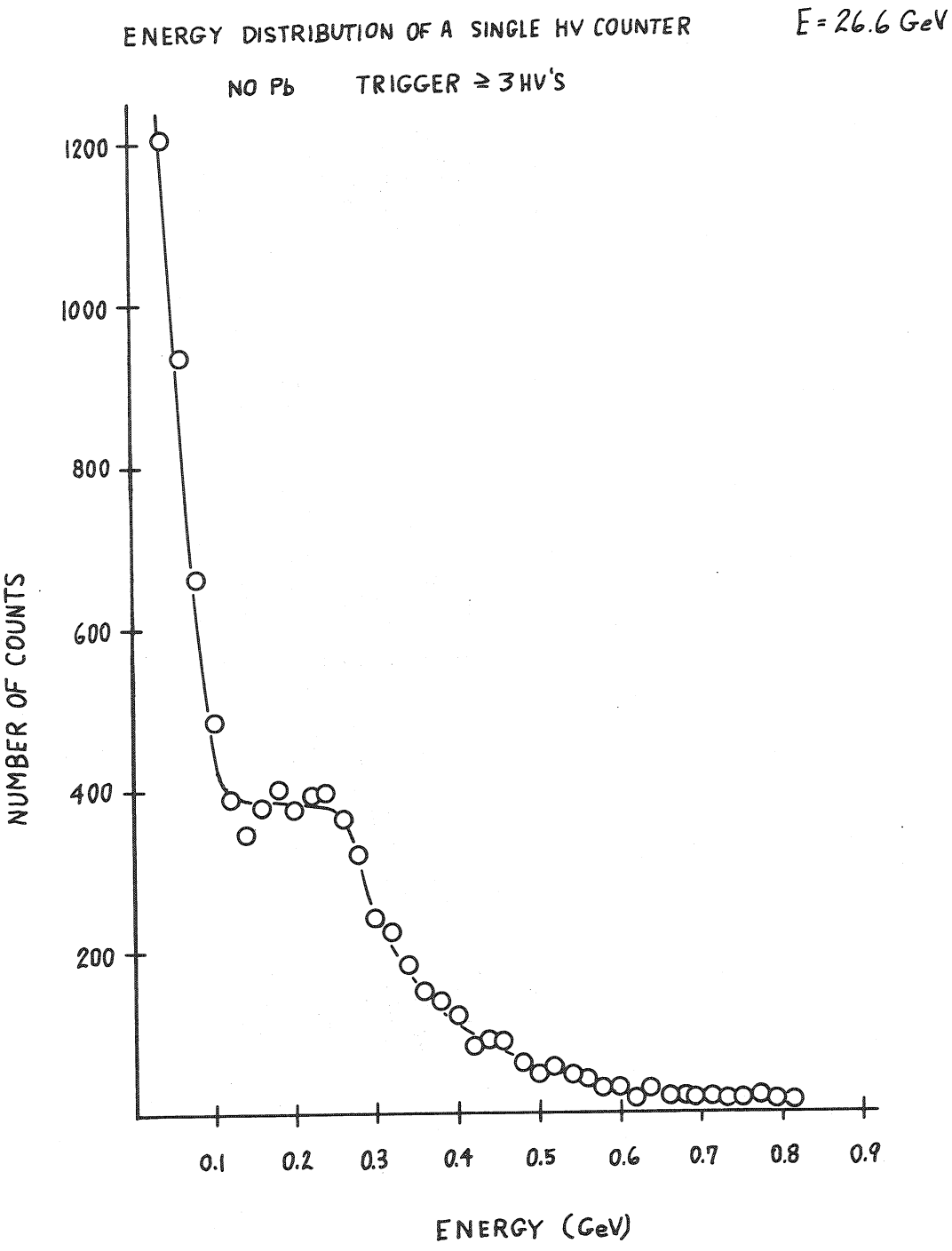
ENERGY DISTRIBUTION OF A SINGLE HV COUNTER
E = 26.6 GeV
NO Pb
TRIGGER ≥ 3 HV'S
NUMBER OF COUNTS
1200
1000
800
600
400
200
0.1
0.2
0.3
0.4
0.5
0.6
0.7
0.8
0.9
ENERGY (GeV)

Fig. 9

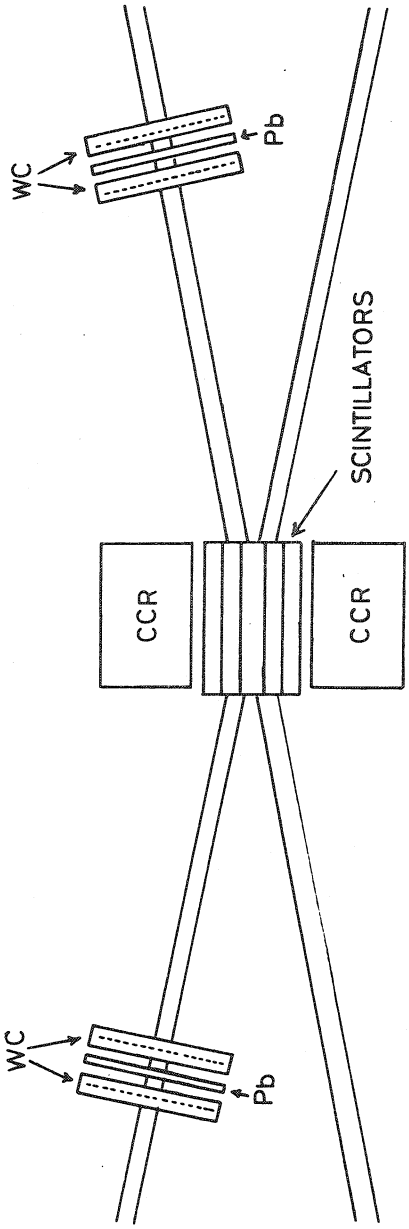

Fig. 10

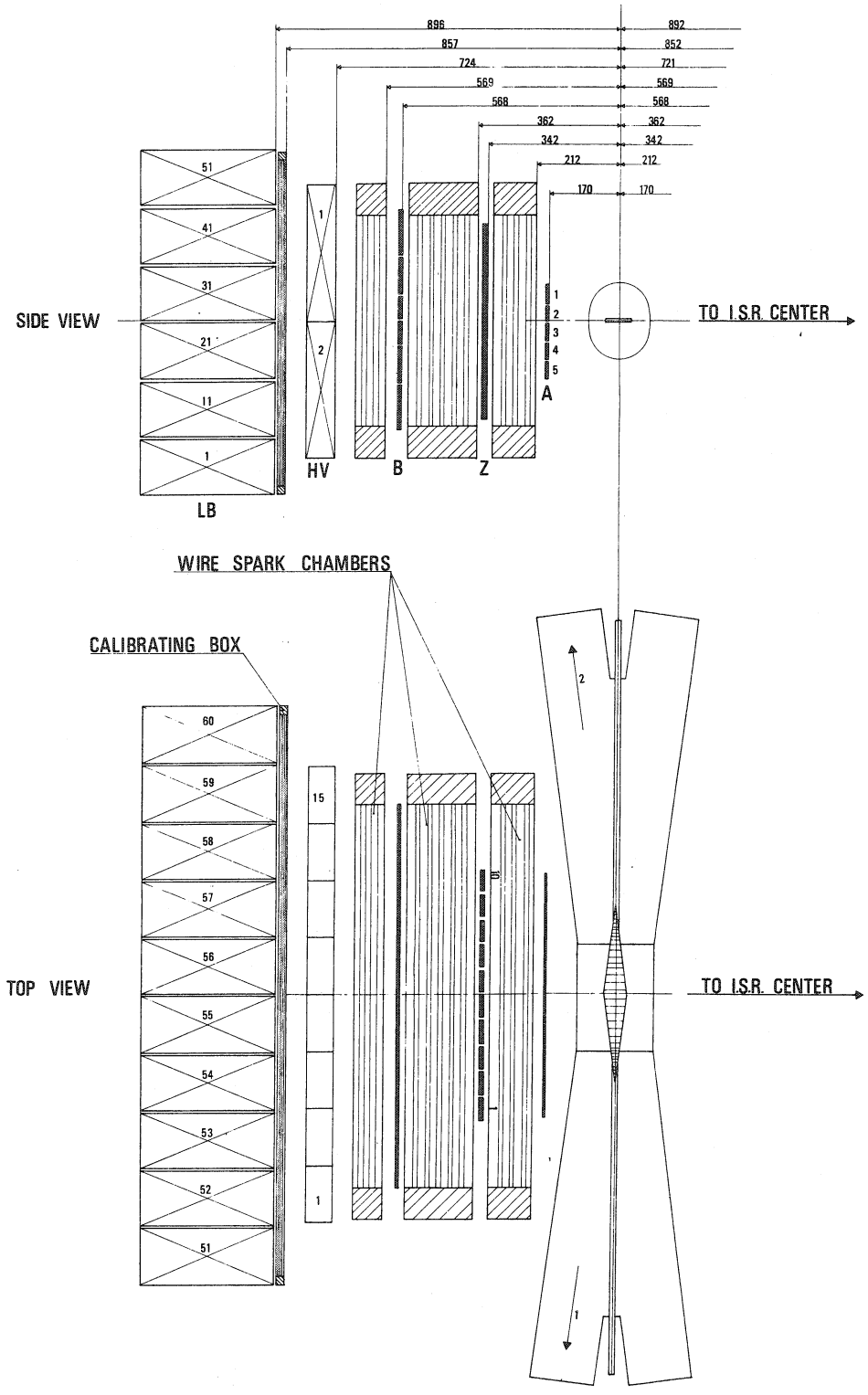
896
892
857
852
724
721
569
569
568
568
362
362
342
342
212
212
170
170
51
41
31
21
11
1
1
2
HV
B
Z
A
1
2
3
4
5
SIDE VIEW
TO I.S.R. CENTER
LB
WIRE SPARK CHAMBERS
CALIBRATING BOX
60
59
58
57
56
55
54
53
52
51
15
1
2
1
TOP VIEW
TO I.S.R. CENTER

Fig. 11

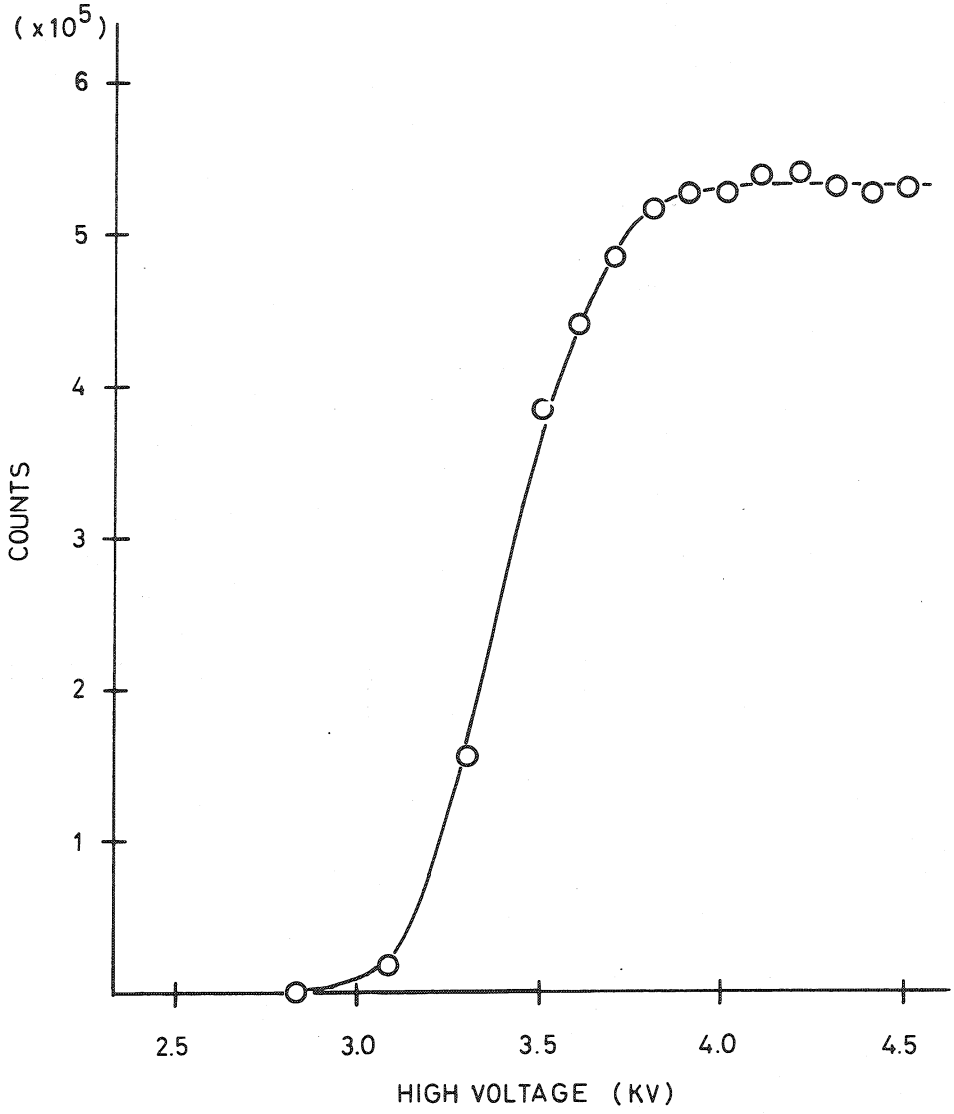

Fig. 12

APPENDIX A

FURTHER INFORMATION ON ASPECTS OF PHYSICAL INTEREST OF MULTIGAMMA EVENTS

1. THE MAIN FEATURES OF THE MULTIGAMMA EVENTS OBSERVED IN COSMIC RAYS

During the period 1953-56, a few events were observed in stacks of nuclear emulsions exposed to cosmic rays at high altitude.

Table A1 summarizes some of the main features of the three typical events, the first one of which was observed by the Chicago Group[2], while the other two were seen by the Torino Group[3]. Several events with the same general features were observed by other authors[4]. Figures A1, A2, and A3 show schematic drawings of these events.

The most interesting results concerning the events of Table A1 can be summarized as follows:

i) No incident charged particle can be observed within 200-300 μ of the axis of the events, with such a direction that it could be considered to be associated with them.

ii) The number of pairs materializing at a given distance increases approximately linearly, reaching a large value in one radiation length (L_{rad} = 2.5 cm).

iii) The energies of the pairs were estimated by one or other of the following two methods:

a) when possible by measuring the energy of each electron from multiple scattering;

b) from the opening angle of the pair, under the assumption that this had its minimum value (so that the two electrons had the same energy). Table A2 shows the results of measurements of this type for the Chicago event. Similar results were obtained for the other events.

The following conclusions were reached by the various authors:

a) Result (ii) excludes the interpretation of these events in terms of usual electromagnetic cascade showers.

b) Nuclear processes with the emission of a large number of π^0 seems also to be excluded. Apart from the fact that the probability that a sufficient number of π^0 are produced with no accompanying charged particles, the high collimation ($< 10^{-3}$ rad) of the bursts would be totally incompatible with energies of the order of 1 GeV as observed for several of the pairs (Table A2).

c) The interpretation of these events seems to require a process in which a large number N_γ of protons are emitted. For the Chicago event, Schein et al. estimate

$$N_\gamma = 21 \pm 3 \ .$$

Similar or larger values are obtained from the other events.

d) From the opening angle of $< 10^{-3}$ rad one can estimate the energy of the primary to be $E_0 \geq 10^{12}$ eV.

It may be interesting to recall that Schein et al. remark in their first letter[2] that the Chicago event would easily be interpreted if it were produced by a high-energy particle annihilating in flight with the emission of only photons of rather low-energy in the c.m.

2. A FEW REMARKS ABOUT THE CREATION AND SUBSEQUENT ANNIHILATION OF DIRAC POLE-ANTIPOLE PAIRS

In order to explain the cosmic-ray events discussed in Section 2.1, Ruderman and Zwanziger[5] have suggested that they could be due to the annihilation of a pair of Dirac magnetic poles produced in a bound state called, in the following, a dipolium. The conjectures of these authors stem from the well-known large value of the magnetic charge of Dirac poles

$$g = mg_0 \qquad \pm m = 1, 2, 3, \ldots \tag{A.1a}$$

$$g_0 = \frac{1}{2}\frac{\hbar c}{e^2} \ ; \qquad e = \frac{137}{2}\, e \ , \tag{A.1b}$$

and from the remark that in order for the vacuum to be stable against spontaneous production of pole pairs at distances down to the Compton wavelength of the lightest hadron ($r_0 \simeq \hbar/m_\pi c^2$), the mass m_g of the poles should satisfy the relationship

$$m_g \geq \frac{m^2}{4}\frac{g^2}{\hbar c} = \frac{m^2}{4}\ 9.6\ \text{GeV} .$$

For distances shorter than r_0, one cannot even speak of pole-antipole separation.

Ruderman and Zwanziger then stress the following points:

1) The coupling constant of Dirac poles to photons is so large,

$$\frac{g^2}{\hbar c} = \frac{m^2}{4}\ 137 , \qquad (A.3)$$

that when, in a high-energy event, a pole and its antipole start to move away, a large number of photons are radiated. Consequently, even at energies much larger than the threshold energy, the pole-antipole pair reaches a maximum separation of the order of $2\text{-}3 \times r_0$ and then falls back, irradiating other photons and finally annihilating; the time involved in the over-all process is of the order of 10^{-22} sec.

2) The number of photons emitted in the production and subsequent annihilation of a dipolium is expected to be very roughly of the order of the coupling constant (A.3), i.e.

$$n_{ph}\frac{g^2}{\hbar c} = \frac{m^2}{2}\ 137 . \qquad (A.4)$$

This general picture not only provides a very reasonable explanation of the anomalous gamma-ray showers discussed in Section 1 of this Appendix, it also explains why, until now, no experimental evidence has been found for the existence of isolated Dirac poles, even if they could actually exist.

It should also be pointed out that the dipolium could be produced in virtual states and could give rise to multigamma events even below the corresponding threshold energy.

Conjecture (1) has been confirmed by Neumeyer and Trefil[10] who have applied the thermodynamical model in order to estimate the probability of producing a pair of poles in a high-energy collision. By taking into account the interaction in the final state, these authors find that the

emission of radiation reduces the probability of production of the poles by two or more orders of magnitude, depending on the values of m and m_g. Doubts can be raised about the use of the thermodynamical model in the case of the dipolium production[1c], but the order of magnitude of the effect of the irradiation of photons should be correct and confirms conjecture (1).

Two more points were discussed in our previous proposal[1c].

a) From the present experimental limits on QED breakdown, limits can be deduced for the production amplitude of the dipolium by a single photon. Are these limits so low that a search for dipolium production at the ISR is completely hopeless?

The problem was treated by Cabibbo and Testa who consider two sets of experimental data: i) the results of the $(g_\mu - 2)$ experiment, and ii) the results obtained at ADONE on the production of muon pairs. The second set of data gives a much lower upper limit[1c], especially if one considers the more recent results[11].

This upper limit is still pretty high

$$\frac{\sigma_X^1}{\sigma_{\mu^+\mu^-}} < 137 \times 4 \ , \qquad \text{(A.5)}$$

where σ_X^1 is the cross-section for production of the dipolium (X) by a single photon, and $\sigma_{\mu^+\mu^-}$ that for the production of pairs of muons.

b) The production cross-section at the ISR was estimated by Cabibbo and Testa by using two different methods.

The first one is based on the comparison of the production (by a single photon) of a pair of Dirac poles

$$p + p \to X + \text{hadrons} \qquad \text{(A.6)}$$

with that of a pair of muons

$$p + p \to \mu^+\mu^- + \text{hadrons} \ . \qquad \text{(A.7)}$$

One can write

$$\left(\frac{d\sigma_{pp\to X+hs}}{dM_X}\right)_{\substack{\text{real or}\\ \text{virtual}}} = K \frac{d\sigma_{pp\to\mu^+\mu^-+hs}}{dM_{\mu\mu}} , \qquad (A.8)$$

where K is a constant of the order of 137, and the cross-section on the right-hand side is obtained by extrapolation of the value observed at the AGS[12] to the ISR energies by some convenient formula.

The results depend very much on the formula adopted for the extrapolation. Besides that used in our previous proposal[13], there are two more recent estimates, both of which provide much lower values. The first one[14] is based on the use of the light-cone approach and represents an improvement with respect to the first paper quoted in Ref. 13. The other[15] is based on the notion of scaling and phenomenological considerations.

c) The second estimate -- based on the Weizsäcker-Williams formula -- gives, on the contrary, a very large cross-section.

All these estimates should, however, be considered with great reservation since they are based on the assumption that the dipolium is produced by a single (virtual or real) photon emitted in the proton-proton collision, while the "effective coupling constant" between a charged particle and a monopole, i.e.

$$\frac{eg}{\hbar c} = \frac{e^2}{\hbar c}\frac{g}{e} = \frac{m}{2} \qquad (A.9)$$

is always of the order of one. Therefore one can expect that processes taking place via the exchange of 2, 3, ... photons should have an amplitude that is not much smaller than that pertaining to a single-photon exchange.

3. A FEW POINTS OF INTEREST IN THE EMISSION OF GAMMA-RAYS THROUGH THE DECAY OF π^0 (AND OTHER PARTICLES) PRODUCED IN p-p COLLISIONS

The interest of the problem is duly stressed in various excellent reports on the multiple production of secondary particles in high-energy collisions[16-19]. Here only a few remarks are collected in order to remind one of the kind of information that can be derived from experiments of the type proposed below, even in the case that no unusual multigamma events were observed. At the same time, these remarks provide the justification for our desire to increase, as much as possible, the solid angle covered by the gamma-ray detector.

In this discussion two simplifying assumptions will be made merely for the sake of clarity: the first one is that only pions are produced in p-p collisions, while we know that the frequencies of production of kaons and antiprotons at the ISR are of the order of 10% and 2.5% [19].

The second simplification consists in discussing the problem as if the π^0 were observed directly, while only the corresponding decay gamma-rays are actually recorded. The relationship between the angular distributions and spectra of the parent π^0 and the daughter gamma-rays complicate the problem, which, however, can be treated by well-known standard methods.

In an ideal experiment the detector would cover the whole solid angle so that the following quantities could be measured for a few values of the c.m. energy:

i) the average multiplicity $\overline{n_0}$ of π^0 produced;

ii) the frequency of production of n_0 neutral pions and its correlation with the production of n_{ch} charged particles;

iii) the density and the correlation function for emission of two pions as they are defined, for example, by Wilson[16].

It may be useful to add a few words about point (iii), i.e. the distribution of the multiplicities $n_{0,ch}$, because such a problem is also directly connected to that of the background of multigamma events from which the possible unusual events should be disentangled.

The problem has been studied by various authors through the analysis of the existing data on the observed total number of charged particles

emitted in high-energy collisions[17,20,21]. The Polish authors[20] find that the n_{ch} distribution deviates appreciably from the Poisson law

$$P(n,\bar{n}) = \frac{\bar{n}^n}{2} e^{-\bar{n}} \quad . \tag{A.10}$$

Apparently this behaviour is mainly due to the presence of one or two protons in the final state. Wang[21] obtains the best fit of the charged pions' frequency distributions assuming that the production of pairs of $\pi^+\pi^-$ is Poissonian. This law could be a consequence of "local charge conservation" which, however, is incorporated in many theoretical models.

Among these one can recall a model based on the assumption that hadrons are composed of a number of sub-units[22], the multiperipheral bootstrap model of Chew and Pignotti[23], which gives a Poissonian law for the observed pion production.

Another model that can be mentioned here is that of Ballestrero et al.[24], who obtain for the charged pions the Furry distribution[25]

$$F(n,\bar{n}) = \frac{1}{\bar{n}} \left(1 - \frac{1}{\bar{n}}\right)^n \qquad n = 0,\ 1,\ 2,\ \ldots \tag{A.11}$$

This is a multiperipheral model where the four-momentum of the produced pions is assumed to be negligibly small with respect to that of the incident particles.

Finally, Quigg, Wang and Yang[26] speculate on the fluctuations of the multiplicity in the fragmentation of hadrons in high-energy collisions, arriving at a few qualitative guesses. Among these, one may recall the fact that the multiplicity of the fragmentation of the two hadrons should not be much correlated. In particular,

$$\frac{\left(\overline{n_{ch}^R} \cdot \overline{n_{ch}^L}\right)}{\overline{n_{ch}^R} \cdot \overline{n_{ch}^L}} \xrightarrow{E_{cm} \to 1} 1 \ ,$$

where R and L stand for "left" and "right" and refer to the two hemispheres within which the fragments of the incoming particles move. Similar considerations hold for neutral fragments.

Table A1

Main features of typical multigamma events

	Exit angle (degrees)	Angle to emulsion surface [a] (degrees)	Total length (cm)	No. of pairs observed	Half-cone angle of burst (rad)
Chicago 1	16	7.5	3.30	16	$\sim 2 \times 10^{-4}$
Torino 1	61	31	2.45	14	$\lesssim 10^{-3}$
Torino 2	32	16	4.68	24	$\lesssim 10^{-3}$

a) The energy evaluation of the electron pairs (Table A2) is more reliable for small values of the angle of the shower axis to the emulsion surface.

Table A2

The first 16 pairs in narrow photon shower. The radial distance is the distance from the pair origin to the median of the electrons at the pair's point of origin. E_1, E_2 are the measured energies of individual electrons. E is the total energy of the photon. The estimate of E for pairs 6, 7, 9, 9 is made from the distance the pair goes before becoming resolvable into individual tracks.

Pair	Distance to point of conversion (μ)	Radial distance (μ)	E_1 (MeV)	E_2 (MeV)	E (MeV)
1			400 ± 160	100 ± 40	500 ± 165
2	2020	1	350 ± 140	300 ± 120	650 ± 330
3	4440	12	350 ± 140	550 ± 220	900 ± 260
4	13 100	3	100 ± 40	800 ± 320	900 ± 325
5	13 350	23	500 ± 200	150 ± 60	650 ± 210
6	15 750	10			> 5000
7	15 770	3			> 5000
8	19 900	1			> 20 000
9	21 600	2			> 20 000
10	27 000	6			
11	27 200	8			
12	29 800	2			
13	30 800	4			
14	31 100	2			
15	31 400	26			
16	33 300	16			

Figure captions

Fig. A1 : Narrow shower of pure photons. Sections at arbitrary intervals to show development of shower. Note pair starting in last section.

Fig. A2 : Projected points of origin and opening angles of the pairs of event To. 1. The lateral slow pairs originate on tracks of the preceding pairs that have been deviated.

Fig. A3 : Projected points of origin and opening angles of 23 pairs of event To. 2. Pair No. 8 is probably a trident on a track of pair No. 2 and it is not drawn in this figure.

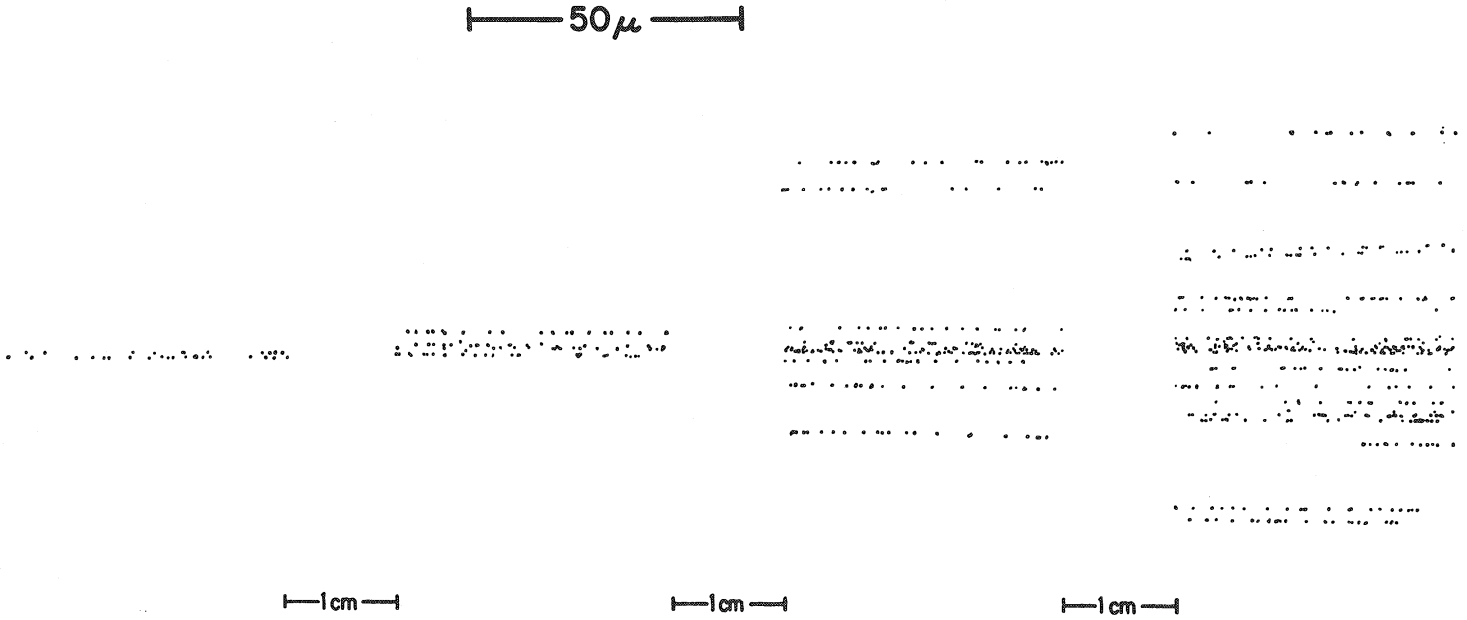

Fig. A1

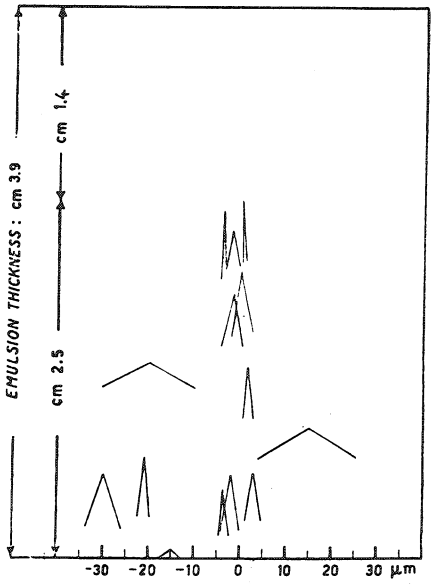
EMULSION THICKNESS : cm 3.9
cm 1.4
cm 2.5
-30 -20 -10 0 10 20 30 µm

Fig. A2

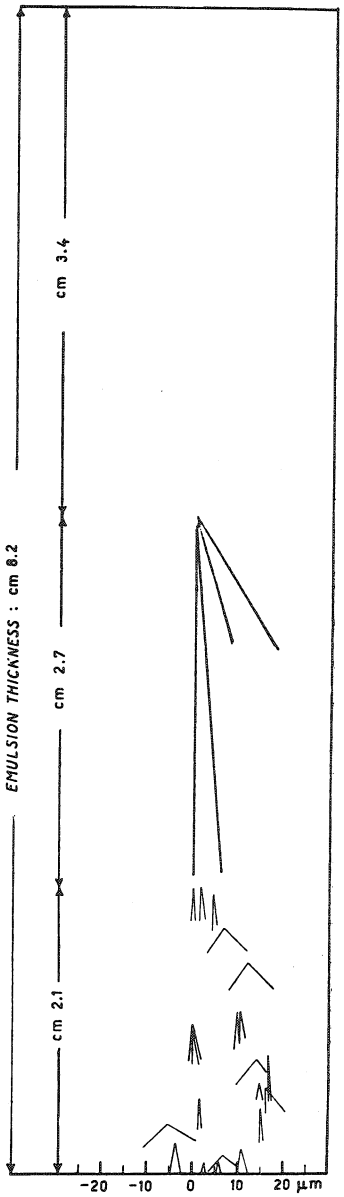
EMULSION THICKNESS : cm 8.2
cm 3.4
cm 2.7
cm 2.1
-20 -10 0 10 20 µm

Fig. A3

APPENDIX B

SIMPLE MODELS OF MULTIPLE PRODUCTION OF SECONDARY PARTICLES

Various approaches can be followed for interpreting the results of experiments of the type considered in this proposal. One of these is based on the construction of simple models, the results of which can be compared with the experiments.

In this Appendix, two very simple models are presented. They allow the derivation of a number of statistical distributions of the counters fired in each multigamma event, which can be compared with the experimental results. The more or less satisfactory agreement (or disagreement) provides information that is very useful for the construction of more elaborate models.

The first model presented here is indicated as Model 0 (zero) because it takes into account only the main geometrical features of the experimental set-up, and provides information only on the number of fired counters, without the introduction of any physical law except that the number of particles fluctuates according to the Poisson law.

The second model, called Model 1, contains the simplest possible assumptions, about the spectra and angular distributions of the secondary particles. These distributions are taken from the experimental results obtained from the observation of a single particle produced at the ISR, operated at the same energy. It does not contain correlations (in angle and/or energy) of any type. Other models are in preparation.

1. MODEL 0: STATISTICAL CONSIDERATIONS OF A PURELY GEOMETRICAL NATURE ON THE DETECTION OF MANY PARTICLES PRODUCED IN SINGLE HIGH-ENERGY EVENTS

Case 0.1: Number of particles N fixed

Let us assume that the particles N are distributed uniformly, with no correlation of any type, over the region covered by the detectors d. Under the assumption that all the detectors have the same probability of being triggered, the probability of having: N_1 particles in detector 1, N_2 particles in detector 2, ..., N_d particles in detector d, is given by the Bernouillian distribution

$$P_N(N_1 \ldots N_d) = \frac{N!}{N_1! \ldots N_d!} \left(\frac{1}{d}\right)^N , \qquad (B.1)$$

where

$$0 \leq N_i \leq N \; ; \quad \sum_1^d{}_i \; N_i = N \; . \qquad (B.2)$$

The probability that only the first n detectors are fired is obtained by introducing into Eq. (B.1)

$$N_i = 0 \quad \text{for } i \geq n + 1 \; ,$$

and summing with respect to $1 \leq i \leq n$ with

$$1 \leq N_i \leq N - n + 1 \; ; \quad \sum_1^n{}_i \; N_i = N \; , \qquad (B.3)$$

i.e.

$$P'_{N,d}(n) = \left(\frac{1}{d}\right)^N \sum_1^{N-n+1}{}_{N_i} \frac{N!}{N_1! \ldots N_n!} \; , \qquad (B.4)$$

the sum being extended to all partitions of N for which the indicated limits are satisfied.

The probability $P_{N,d}(n)$ that only n detectors, chosen at random, are fired is given by

$$P_{N,d}(n) = \frac{d!}{(d-n)!\,n!} P'_{N,d}(n) = \left(\frac{1}{d}\right)^N \frac{d!}{(d-n)!\,n!} \sum_1^{N-n+1}{}_{N_i} \frac{N!}{N_1! \ldots N_n!} \; . \qquad (B.5)$$

In order to compute the sum on the right-hand side of this expression, it is convenient to perform the substitution

$$\begin{aligned} N'_i &= N_i - 1 \\ 0 \leq N'_i &\leq N - n \\ \sum_1^n{}_i \; N'_i &= N - n \; . \end{aligned} \qquad (B.6)$$

Thus Eq. (B.5) becomes

$$P_{N,d}(n) = \left(\frac{1}{d}\right)^N \frac{d!}{(d-n)!n!} \frac{N!}{(N-n)!} \sum_{N_i'}^{N-n} \frac{(N-n)!}{(N_1'+1)!\ldots(N_n'+1)!} =$$

$$= \left(\frac{1}{d}\right)^N \frac{d!}{(d-n)!n!} \frac{N!}{(N-n)!} \int_0^1 dt_1 \ldots \int_0^1 dt_n (t_1 + \ldots + t_n)^{N-n} . \tag{B.7}$$

The integral of order n on the right-hand side of Eq. (B.7) can be calculated analytically. Thus one obtains

$$P_{n,d}(n) = \left(\frac{1}{d}\right)^N \frac{d!}{(d-n)!n!} \sum_0^n {}_i (-1)^i \frac{n!}{(n-i)!i!} (n-i)^N . \tag{B.8}$$

In the last two expressions the factorial of any negative number is taken equal to infinity.

One can easily verify that the expression (B.8) is identical to zero for $n \geq N$.

Case 0.2: The particle distribution is assumed to be Poissonian

If the multiplicity of the particles is not always N but fluctuates according to the Poisson law in the region covered by the detectors, around a mean value Δ, the probability that n detectors are fired is given by

$$P_{\Delta,d}(n) = \sum_{0N}^{\infty} \frac{\Delta^N}{N!} e^{-\Delta} P_{N,\Delta}(n) =$$

$$= \frac{d!}{(d-n)!n!} e^{-\Delta} \sum_0^n {}_i (-1)^i \frac{n!}{(n-i)!i!} \sum_{0N}^{\infty} \frac{1}{N!} \left[\frac{\Delta(n-i)}{d}\right]^N$$

$$= \frac{d!}{(d-n)!n!} e^{-\Delta} \sum_0^n {}_i (-1)^i \frac{n!}{(n-i)!i!} e^{\Delta(n-i)/d} . \tag{B.9}$$

Case 0.3: Number of particles fixed, and detectors with efficiency $\eta \leq 1$

Let us denote by K the number of particles produced in a single event, with η the efficiency of detection. The case is included of the detectors d covering the fraction η of the total solid angle, K being the total number of particles emitted over 4π sr.

The probability that n detectors are fired is given by

$$P_{K,d}(n) = \sum_{0}^{K}{}_{N} \frac{K!}{(K-N)!N!} \eta^N (1-\eta)^N P_{N,d}(n) =$$

$$= \frac{d!}{(d-n)!n!} \sum_{0}^{n}{}_{i} (-1)^i \frac{n!}{(n-i)!i!} \left(1 + \frac{n-i-d}{d}\eta\right)^K . \tag{B.10}$$

Case 0.4: The particle distribution is assumed to be Poissonian and the detectors have efficiency η

In this case one has

$$P_{\bar{N},d}(n) = \sum_{0}^{\infty}{}_{K} e^{-\bar{N}} \frac{\bar{N}^K}{K!} P_{K,d}(n) =$$

$$= \frac{d!}{(d-n)!n!} e^{-\bar{N}} \sum_{0}^{n}{}_{i} (-1)^i \frac{n!}{(n-i)!i!} \exp\left[-\bar{N}\left(1 + \frac{n-i-d}{d}\eta\right)\right] . \tag{B.11}$$

The sums appearing in expressions (B.9) and (B.10) can easily be computed. One has

$$P_{\Delta}(n) = \frac{d!}{(d-n)!n!} e^{\Delta(n-d/d)} \left[1 - e^{-\Delta/d}\right]^n , \tag{B.12}$$

where $\Delta = \bar{N}\eta$ in case (B.11).

Thus the expressions (B.9) and (B.11) are identical provided the mean value of the number of particles crossing the detectors is the same.

The generating function of the distribution (B.12) is

$$G(t) = e^{-\Delta}\left[1 + \left(e^{\Delta/d-1}\right)\right]^d . \tag{B.13}$$

The mean value of n is given by

$$\bar{n} = \lim_{t\to 1} \frac{dG}{dt} = d\left(1 - e^{-\Delta/d}\right) . \tag{B.14}$$

In order to compute the variance of the distribution (B.12), one has to recall that

$$\overline{n^2} - \bar{n} = \lim_{t\to 1} \frac{d^2G}{dt^2} = d(d-1)\left[1 - e^{-\Delta/d}\right]^2 , \qquad (B.15)$$

from which it follows that

$$\overline{(\delta n)^2} = d\left[1 - e^{-\Delta/d}\right] e^{-\Delta/d} = \bar{n}\left(1 - \frac{\bar{n}}{d}\right) . \qquad (B.16)$$

The expression (B.12) can also be put in the form

$$P_\Delta(n) = \frac{d!}{(d-n)!\,n!} \left(\frac{\bar{n}}{d}\right)^n \left(1 - \frac{\bar{n}}{d}\right)^{d-n} . \qquad (B.17)$$

Furthermore one has

$$\Delta = -d \cdot \ln\left(1 - \frac{\bar{n}}{d}\right) , \qquad (B.18)$$

from which it follows

$$\sqrt{\delta\{\Delta^2\}} = \frac{\Delta \cdot \bar{n}}{1 - \frac{\bar{n}}{d}} = \sqrt{\frac{\bar{n}}{1 - \frac{\bar{n}}{d}}} . \qquad (B.19)$$

Figures B1 to B6 show a comparison of the results obtained in the run 1687 (circles) with the results of this model (crosses). The curves are drawn only to guide the eye.

2. MODEL 1: MONTE CARLO PROGRAMME FOR SIMULATING MULTIGAMMA EVENTS WITH NO CIRCULATION OF ANY TYPE

Assumptions

1a) Four-momentum conservation is not imposed on the secondary particles since the energy and momentum balance are assured by the final nucleons which (together with a few secondaries) carry about one-half of the total energy and move to such a small angle to escape observation.

1b) The emission of $n_\pm$ charged pions is assumed to be independent of the emission of n_0 neutral pions.

1c) The observed single-particle spectrum measured at the same energy at the ISR,

$$\frac{dN}{dp_T} = B^2 p_T \, e^{-Bp_T} , \qquad p_T = 5.7 \ (GeV/c)^{-1} \tag{B.20}$$

is assumed to hold for any value of the multiplicity. This assumption is reasonable as a first approximation but it has no supporting experimental evidence. On the contrary, correlations between particle spectra are expected to be of the utmost importance.

1d) The angular distribution observed for single $\pi^{\pm}$ emission and tested for single π^0 production is assumed to hold for any value of $n_{\pm}$ and n_0:

$$\frac{dN}{d\Omega} = \frac{dN}{d\phi d \cos\theta} = \frac{a_1}{a_2 + \sin^2\theta} , \qquad \begin{aligned} a_1 &= (0.106 \pm 0.01) \ sr^{-1} \\ a_2 &= (6.31 \pm 4.0) \times 10^{-3} . \end{aligned} \tag{B.21}$$

1e) The multiplicity distribution is assumed to be Poissonian for the production of the pairs of $\pi^{\pm}$ as well as for the π^0, with no correlation between the two distributions. For the average values we have used those given in the report by Sens [19] at the Oxford Conference

$$P(n) = \frac{e^{-\langle n \rangle}}{n!} \, n^{\langle n \rangle} . \tag{B.22}$$

Once a sufficiently large number of events have been generated by means of this programme, they are analysed by means of the same procedure as that used for the observed events, and the results are compared.

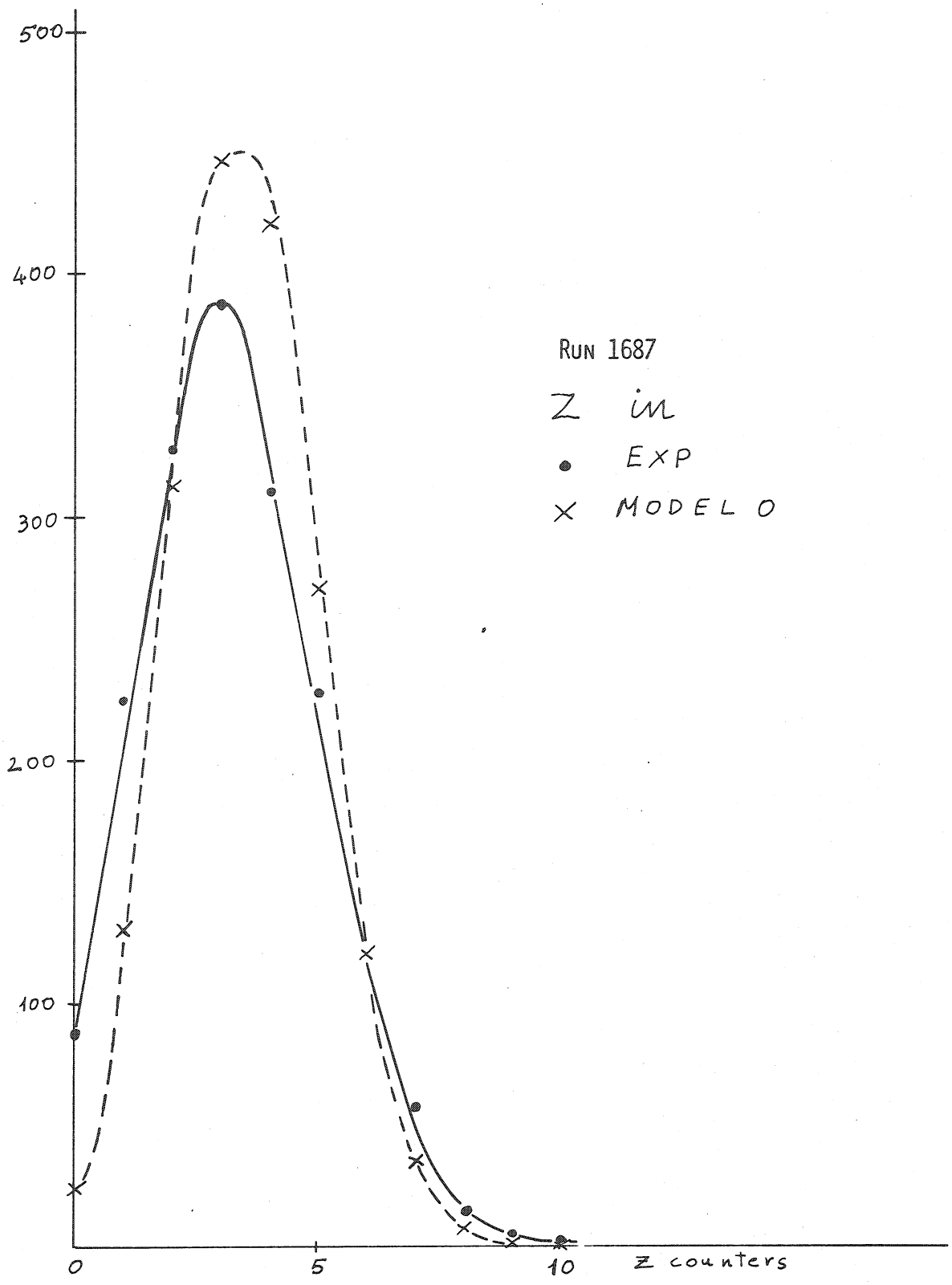

Fig. B1

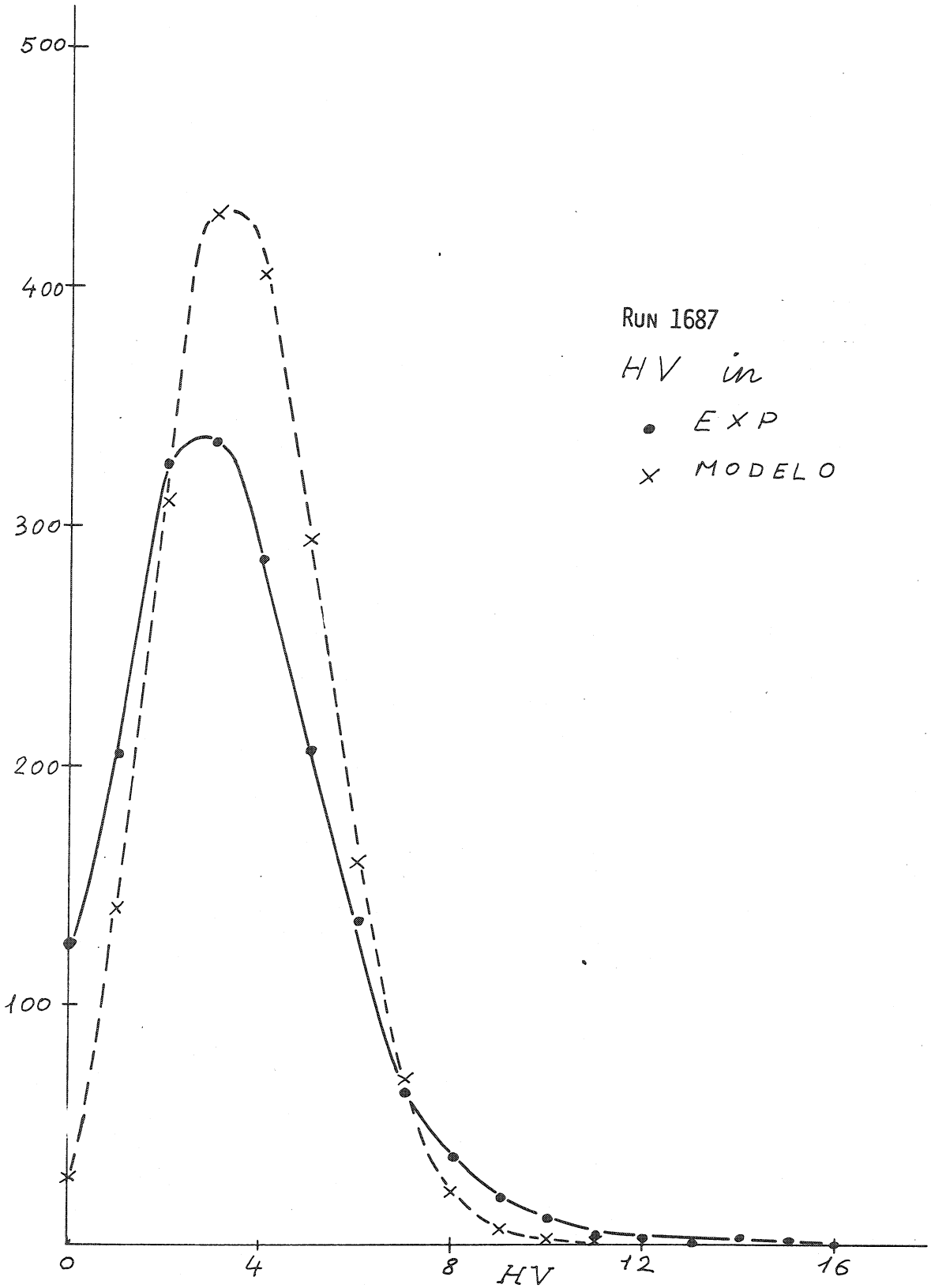

Fig. B2

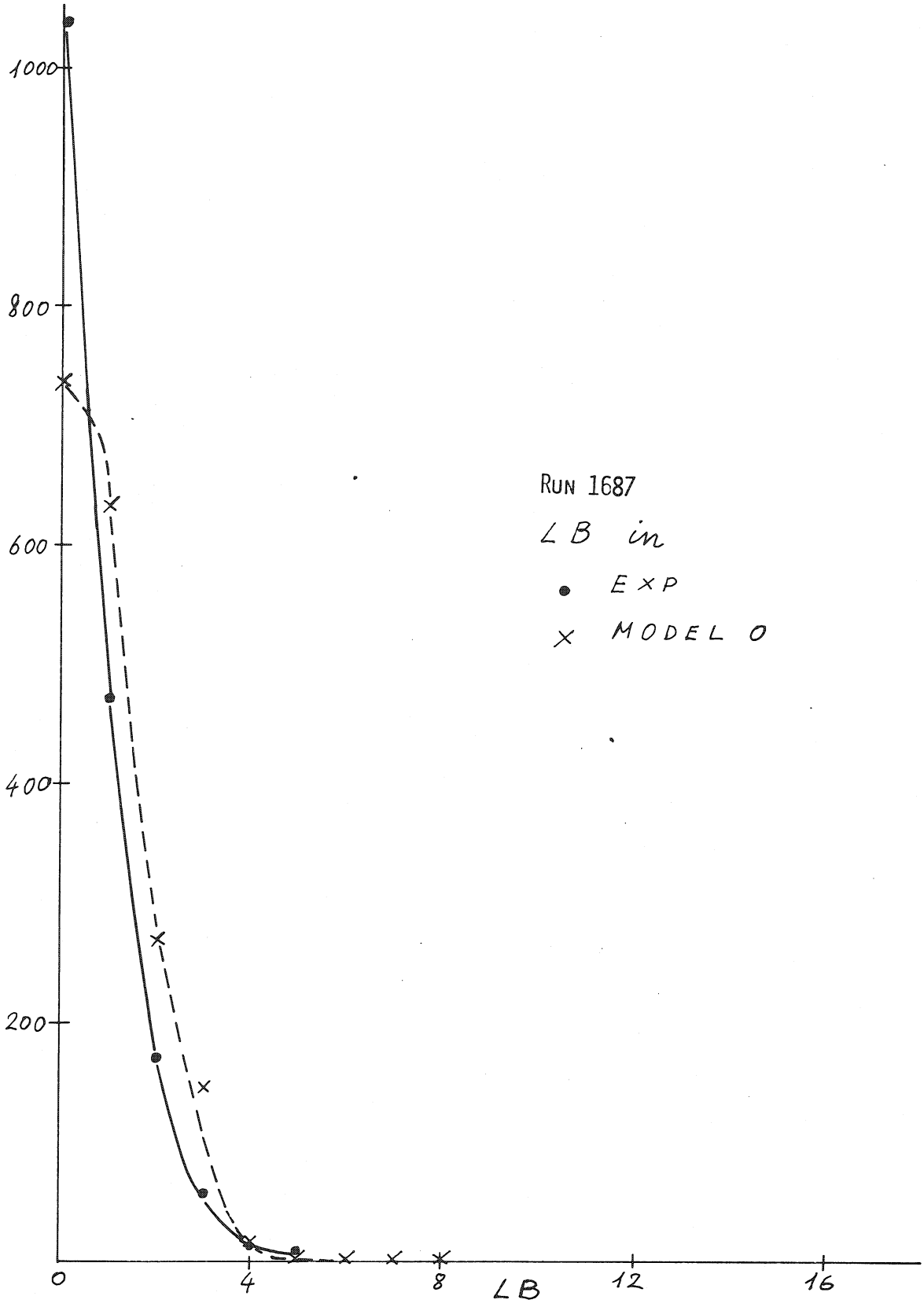

Fig. B3

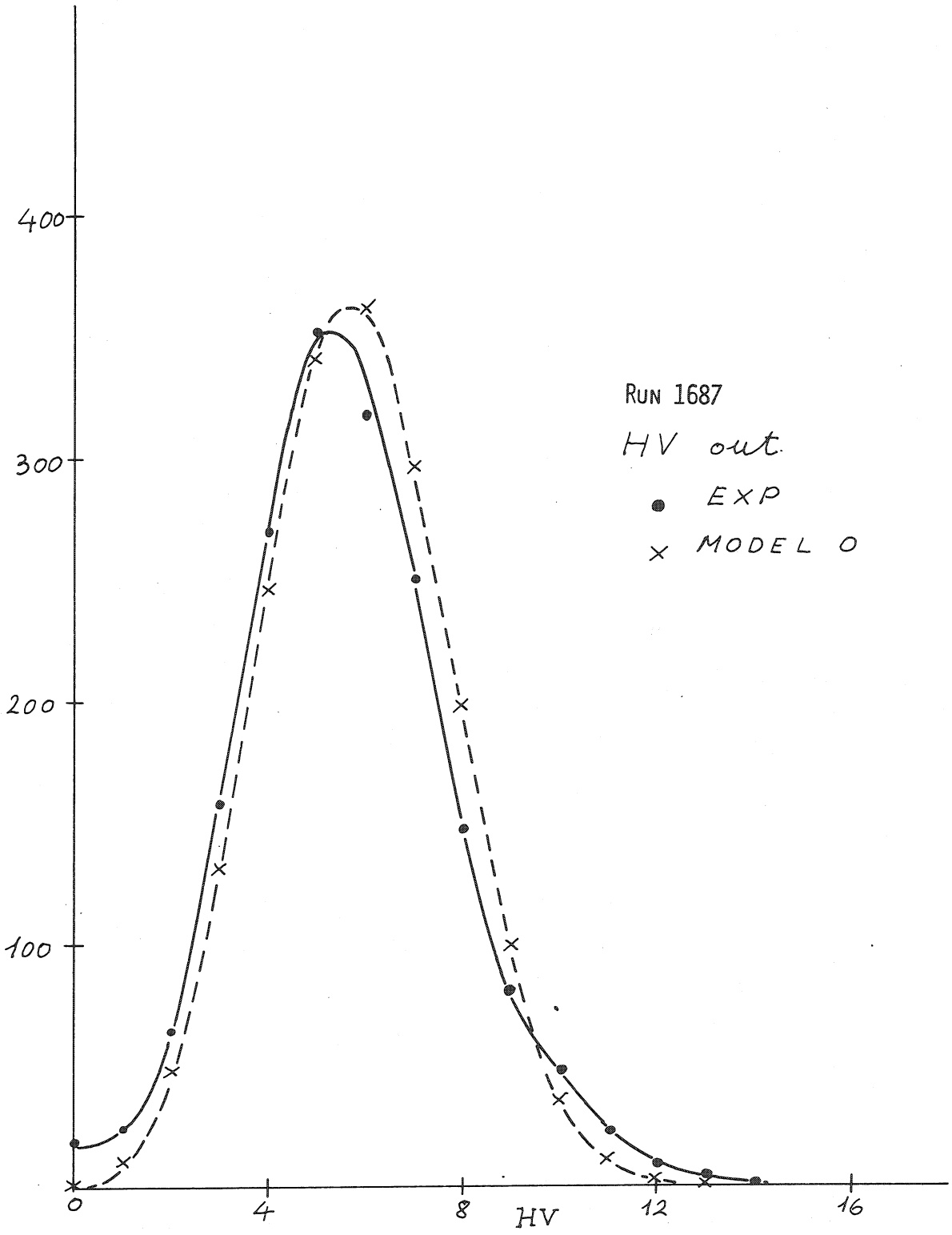

Fig. B4

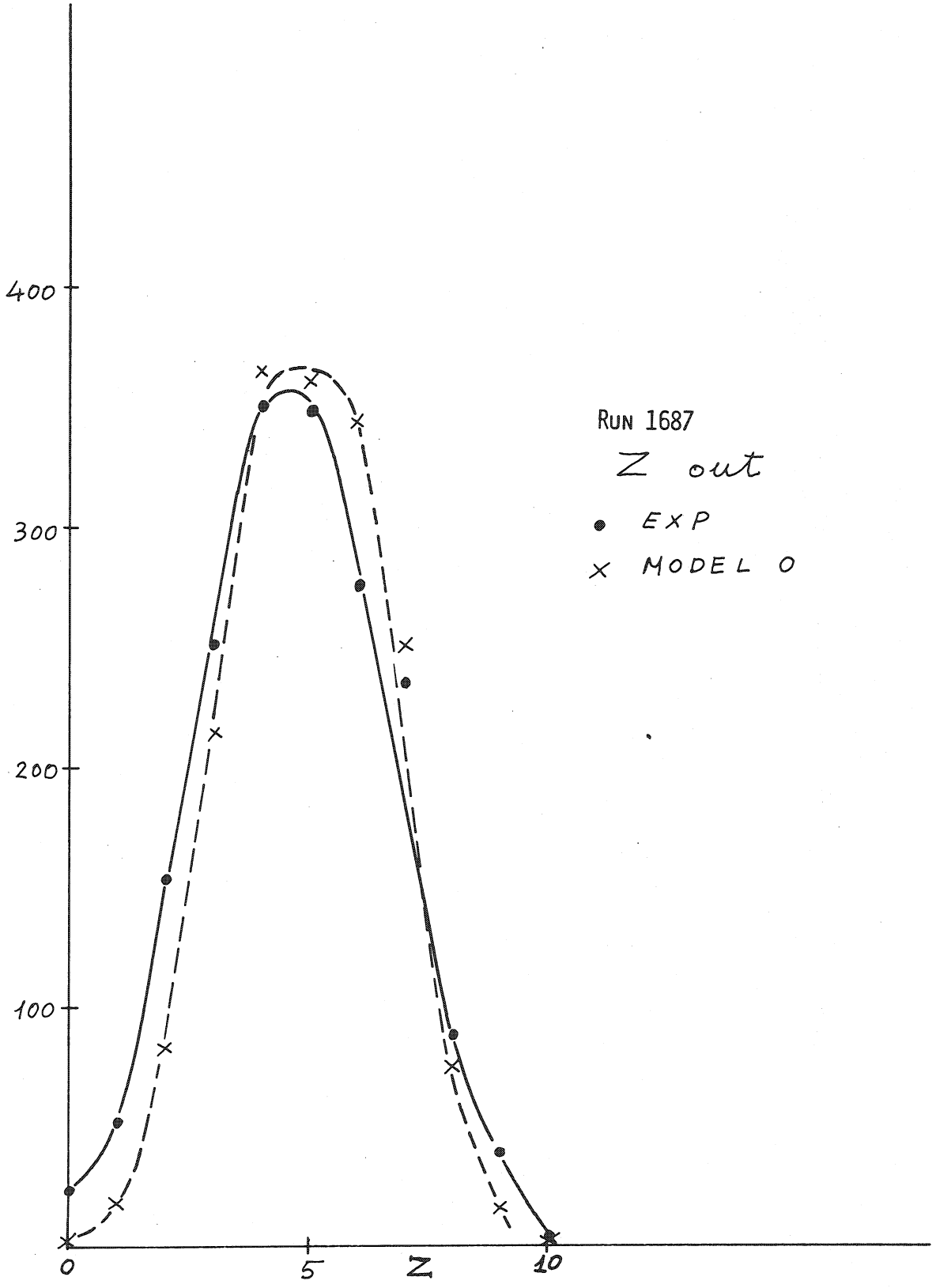

Fig. B5

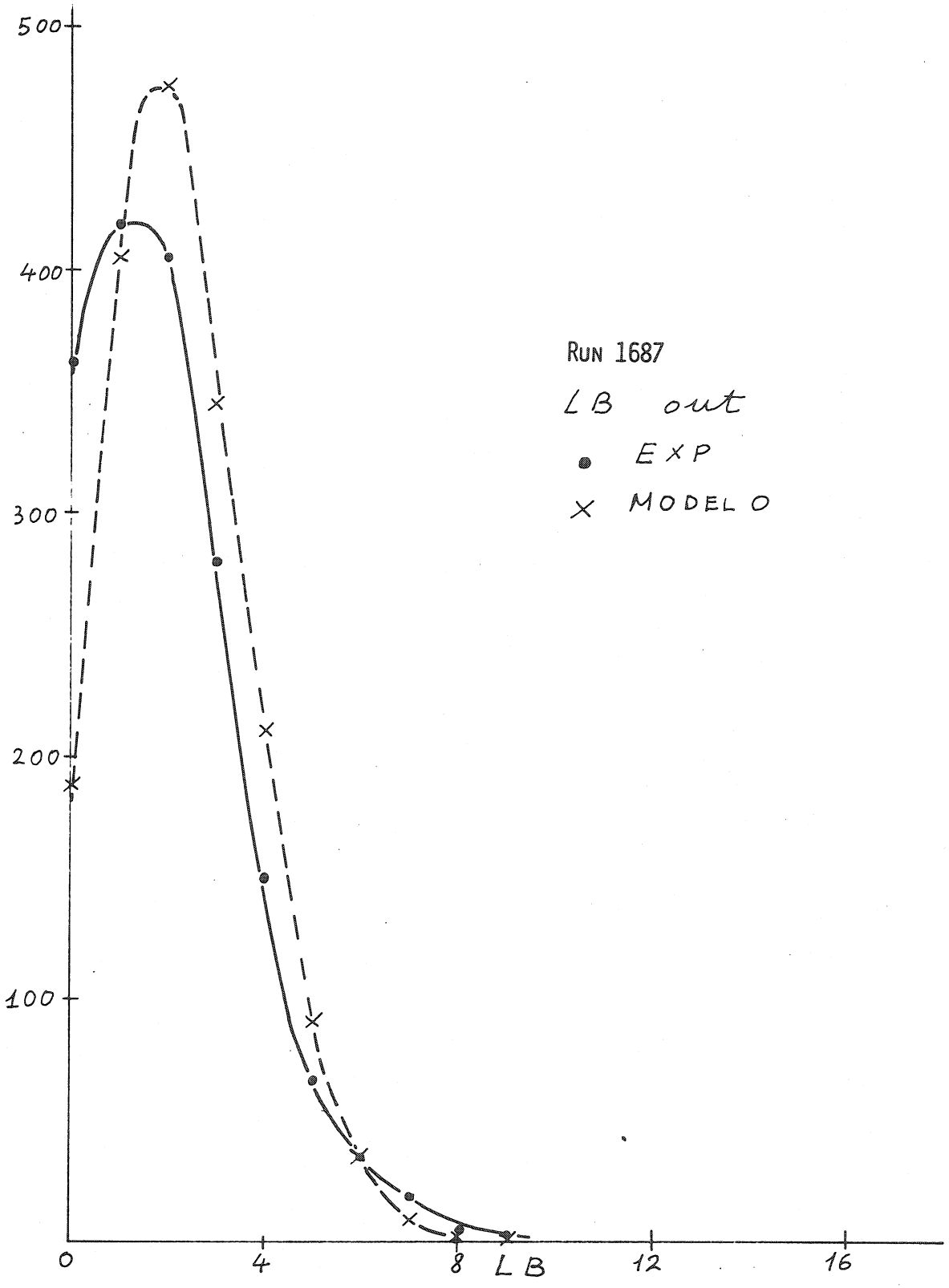

Fig. B6

APPENDIX C

DETAILS OF THE TESTS ON WIRE GROUPING IN A MULTIWIRE PROPORTIONAL CHAMBER (MWPC)

In our proposed exploratory experiment on multigamma production at the ISR, special detectors are required which can measure simultaneously both the number of gamma-rays as well as the number of charged particles covering as much solid angle as possible over the beam interaction region. The simplest and, perhaps, the most versatile and reliable detection system for fulfilling the above requirement is a system of two multiwire proportional chambers with a thin lead converter sandwiched between them. The first chamber measures the charged particles, whereas the second chamber behind the lead converter measures the gamma-rays. Such a system also enables us to determine the space location of the particles and gamma-rays with an accuracy depending on the wire spacing of the individual chambers, thus yielding an angular distribution of these multiple events. Extensive investigations on MWPC and their applications have been carried out by Charpak and his collaborators[8], including the behaviour of various gas mixtures used in the chamber, the wire spacing and chamber efficiency, stability, and many other characteristics.

For obtaining high detection efficiency and ease of operation, a wire chamber with an effective area of 1 m^2 and a wire spacing of 3 mm was constructed. Since the resolution in the space location of the multigamma events does not need to be high in an inherent centre-of-mass system, which is characteristic of a colliding beam machine, much economy can be realized if a number of signal wires can be grouped together, which reduces the number of amplifier + logic channels by a factor equivalent to the number of wires that are grouped together. Otherwise, one such channel would be required by each individual wire. It was decided that an eight-wire grouping would be a good compromise in space resolution and an economy in the cost of the electronics system. Although a seven-wire grouping in smaller size (50 cm × 50 cm) MWPC has been successfully used (with 5 mm spacing and a standard argon-methane gas mixture) at Brookhaven on another experiment[7], and similar wire groupings

have also been tried[8] in comparatively small chambers, no data seem to be available on eight-wire grouping in large chambers such as those having 1 m^2 effective area. A grouping together of such long wires would certainly present a considerably higher effective input capacity, thus reducing appreciably the chamber signal pulse-height. The main purpose of the present investigation on the wire grouping effect is to ascertain to what extent an eight-wire grouping in such a large-size chamber will affect the signal output; and what kind of a simple and economic pre-amplifier with sufficient gain to give an adequately safe signal-to-noise ratio, and to yield a 100% detection efficiency in the chamber, will be required.

A prototype MWPC was designed, constructed, and kindly provided by the CERN NP Division for us to make a thorough investigation of this matter.

1. DESIGN OF THE PROTOTYPE MULTIWIRE PROPORTIONAL CHAMBER

This chamber consists of one signal wire plane with a wire spacing of 3 mm and two high-voltage wire planes of 1 mm wire spacing on either side of the signal wire plane. The distance between the signal plane and each high-voltage plane is 8 mm, and the effective area of the wire chamber is 1 m^2. The body of the chamber is enclosed by a thin Aclar-Mylar window on each side, and a finely meshed wire screen immediately on the outside of the mylar windows serves as an electrostatic shield when properly grounded.

This prototype chamber was first filled with the commonly used argon + CO_2 mixture (80% argon, 20% CO_2), and investigations were made with both radioactive sources (such as ^{55}Fe which emits 5.9 keV X-rays and 230 keV gamma-rays; and ^{90}Sr which emits 546 keV electrons) and 6.5 GeV/c pions at the CERN PS. The effect of adding methylal to the argon + CO_2 mixture was investigated, and the well-known "magic gas" mixture was later used to replace the argon + CO_2 mixture.

A careful study of the behaviour of a single signal wire (two-wire grouping, three-wire grouping, up to eight-wire grouping) was made, and current preamplifiers as well as voltage preamplifiers were tested.

The chamber noise as well as the noise pick-up by the chamber at the PS were also investigated.

2. TESTS WITH RADIOACTIVE SOURCES

Most of the tests shown here were carried out with a well-collimated ^{55}Fe source. Figure C1 shows the electronic circuit arrangement, which consists of an emitter follower at the signal wire output, followed by amplifiers and pulse shaper, etc. Figure C2a shows the pulse-height distribution of the pulses obtained from a single signal wire with all the rest of the wires grounded when the chamber was filled with the argon + CO_2 mixture. The large peak at the right-hand side shows the 5.9 keV X-ray line, whereas the small peak at the left-hand side could be due to a combined effect of background and induced current effect from neighbouring wires. Figure C2b shows the output from two-wire grouping (i.e. two adjacent wires connected in parallel) which is similar to Fig. C2a but with a lower pulse output as indicated by the shifting of the 5.9 keV peak to the left. This is understandable because of the increase in effective input capacity of the emitter follower circuit. Figures C2c and C2d show the signal output distribution from four-wire grouping and eight-wire groupings, respectively. Figures C2e and C2f show similar results from three-wire and five-wire groupings, respectively. All these results were obtained with a high voltage of 3 kV on the chamber, and the general indication is that the height of the main peak seems to decrease for each increasing number of wires grouped together. However, there also appears to be additional bumps at higher pulse heights when the number of wires in a wire grouping is increased, especially in the five-wire grouping as shown in Fig. C2f. One possible conjecture of this phenomenon may be that it is due to a complex summation of the induced current effect produced in the neighbouring wires. Although a number of other tests were performed (but are not mentioned here) which tend to support this conjecture, a real understanding of this phenomenon requires further studies in this respect. However, as the high voltage of the chamber is raised to a sufficiently high value, such structures will tend to merge into a single broad peak.

2.1 Single-wire plateau

Without the use of a counter telescope and with the collimated ^{55}Fe source centred on the single signal wire to be measured with the rest of the wires grounded, a high-voltage plateau curve is shown in Fig. C3, where the input impedance of the emitter follower is 1 kΩ. Figure C4 shows the signal output voltage in mV at the output of the emitter follower as a function of the high voltage.

2.2 Eight-wire grouping plateau

A high-voltage plateau curve for eight-wire grouping is shown in Fig. C5a where a pulse shaper was used, as in the above. Figure C5b shows that a much wider plateau can be obtained if a limiter is used; this is because the shaper has a built-in differentiation input circuit, whereas the limiter has a d.c. coupled input circuit. The signal output as a function of the high voltage on the chamber is shown in Fig. C6, and it is considerably smaller than that from a single wire as shown in Fig. C4.

Tests with a ^{90}Sr electron source have also been made, but these results will not be described here.

3. TESTS IN THE PS PION BEAM

The prototype chamber was placed in a 6.4 GeV pion beam of the Λ^0 group (University of Rome and Rutherford Lab. group) at the PS. Two small scintillation counters S_1 and S_2 were set up as the beam-defining counter telescope as shown in Fig. C7, where A represents either an emitter follower or a preamplifier. Here A is directly attached to the wire chamber.

Three different gas mixtures have been tried in the wire chamber and two different types of preamplifiers were investigated. The latter include voltage amplifiers of different amplifications and current amplifiers of different impedances and gains. Most of the tests carried out here, unless otherwise stated, were made with an emitter follower.

3.1 Tests with argon + CO_2 gas mixture

At a voltage of 3.2 kV on the high-voltage planes of the chamber and with an eight-wire grouping centred in the pion beam, the chamber

efficiency for detecting 6.4 GeV/c pions as a function of amplifier gain is shown in Fig. C8. The dotted curve shows the percentage of accidentals, which is very small. With the gain of the amplifier at 70, the chamber reaches 100% efficiency at the operated high-voltage value of 3.2 kV. The average signal pulse-height from the eight-wire grouping due to 6.4 GeV/c pions is $\sim$ 1.5 mV at the output of the emitter follower. The width (FWHM) of such pulses is $\simeq$ 150 nsec. The total current of the chamber when the pion beam passes through the chamber is 3 μA. The pion beam intensity is $\sim 3 \times 10^4$/sec.

The signal voltage can be increased to 2 mV if the high voltage in the chamber is increased to 3.25 kV, but the total chamber current also increases to 5 μA.

3.2 Tests with argon + CO_2 + methylal

The argon + CO_2 gas mixture was bubbled through methylal liquid, which was kept at 0°C. The addition of methylal seemed to improve the chamber performance to a certain extent in that the high voltage can be increased to 3.7 kV without causing excessive dark current in the chamber. However, the signal pulse-height has not been noticeably improved for the same high voltage.

3.3 Tests with the "magic gas" mixture

Using the "magic gas" mixture, i.e. argon + freon + isobutane + methylal, as first suggested by Charpak et al.[8], eight-wire grouping tests with and without the beam-defining counter telescope were performed. With the amplifier gain set at 30, the high-voltage plateau curve taken without the counter telescope is shown in Fig. C9a, and that taken with the counter telescope is shown in Fig. C9b. The average pulse height of the signals at 3.8 kV is 15 mV at the output of the emitter follower, and the maximum pulse height is $\sim$ 40 mV; whereas the average pulse height at 4.0 kV is 22 mV and the maximum pulse height is $\sim$ 70 mV. Figure C10 shows the average pulse height as a function of high voltage.

3.3.1 Tests with various types of preamplifiers designed by the CERN-NP electronics group

Voltage preamplifiers[9] with two different amplifications were tried. The input impedance of these preamplifiers is $\sim$ 1 kΩ. The noise pick-up

problem at the PS in such a large-size chamber with eight wires grouped and with 1 kΩ input impedance is sufficiently serious that extensive shielding and grounding studies are required in order to operate such a chamber in a way that is reliably free from noise pick-up; thus low-impedance current amplifiers would be much more preferable under these operating conditions. Consequently, two such current preamplifiers, one high gain and one low gain, were designed and constructed by the NP Electronics Group.

i) Test of low-gain current preamplifier

When feeding into the receiver-trigger-memory module, the current threshold I_T is 4.2 μA, the threshold voltage V_T is 0.85 mV, and the input impedance Z_{in} is 200 Ω. The high-voltage plateau curve of the wire chamber using this amplifier is shown in Fig. C11.

ii) Test of high-gain current preamplifier

The threshold of this circuit is 2.2 μA and the input impedance Z_{in} is 300 Ω. The high-voltage plateau curve is shown in Fig. C12. The amplitude of the signal pulse at the output of this current amplifier is approximately 200 mV at 4 kV with a pulse width of ∿ 100 nsec, and the signal amplitude increases to ∿ 320 mV at 4.2 kV with a pulse width of ∿ 160 nsec.

3.3.2 *Investigations on the wire chamber noise and noise pick-up*

The high-gain current preamplifier described in Section 3.3.1 (ii) was used throughout this investigation. The preamplifier board was mounted on the wire chamber with a long cable (50 m) consisting of twisted wire pairs, which brought the signal pulses to the receiver-trigger-memory module[7] for recording and analysis by using the so-called FAST-OR. The noise pick-ups were measured and analysed at the end of the 50 m cable. The identification of the sources of the noise pick-ups was made by shorting the input and output sides of the preamplifier; by disconnecting the preamplifier input from the signal wires of the chamber but leaving the ground connected to the chamber, and so forth. It appears that the noise pick-ups at the PS can be grouped into three categories, namely:

a) Noise pick-up from the accelerator, which consists of spikes of $\sim$ 10 μsec wide and 40 mV maximum amplitude with a frequency of $\sim$ 100 Hz.

b) Intermittent RF pick-up of $\sim$ 5 MHz in frequency and $\sim$ 20 mV in amplitude. These may possibly be due to the research telephone transmissions.

c) Immense spikes of $\sim$ 400 mV in amplitude. These are due to the firing of spark chambers in the vicinity.

d) Chamber noise. The noise pulses from the chamber were measured when the internal beam of the PS was on but no spark chambers were operating nearby. The measured pulses were extrapolated to the full chamber when all the wires were connected in eight-wire groups. The number of noise counts per sec per chamber as a function of the high voltage on the chamber is shown in Fig. C13. At the operating voltage of, say, 4 kV the total noise count is $\sim 3 \times 10^3$ per sec per chamber.

Tests showed that the amplitudes of the noise pulses described in (a) and (b) were well below the threshold of the receiver-trigger-memory modules, so they did not affect the operation of such a wire chamber system. The spark chamber pulses described in (c) can be gated out easily. The chamber noise described in (d) is of such a low rate as compared with the high resolution of the beam-beam coincidence requirement, that it is of no significance in the proposed operation.

4. CONCLUSIONS

a) The detection efficiency of the wire chamber filled with the "magic gas" and using a high-gain current preamplifier is 100% at 4 kV.

b) The effects of the chamber noise and all other noise pick-ups can be easily eliminated in the present design.

Figure captions

Fig. C1 : Block diagram of electronics used in the chamber tests.

Fig. C2 : Pulse-height distribution using an ^{55}Fe source:

a) single wire
b) two-wire grouping
c) four-wire grouping
d) eight-wire grouping
e) three-wire grouping
f) five-wire grouping.

Fig. C3 : Voltage plateau for a single wire.

Fig. C4 : Dependence of emitter follower output on chamber voltage for a single wire.

Fig. C5 : Voltage plateaux for eight-wire grouping:

a) with a shaper
b) with a limiter.

Fig. C6 : Dependence of emitter follower output on chamber voltage for an eight-wire grouping.

Fig. C7 : Set-up used for testing the chamber in a pion beam at the PS.

Fig. C8 : Dependence of detection efficiency for 6.4 GeV/c pions on the amplifier gain (solid curve).
Dependence of accidental counts on amplifier gain (dashed curve).

Fig. C9 : a) High-voltage plateau using "magic" gas and no beam telescope (eight-wire grouping).

b) High-voltage plateau using "magic" gas and the beam telescope (eight-wire grouping).

Fig. C10 : Dependence of the average pulse height from the emitter follower on the chamber voltage (magic gas and eight-wire grouping).

Fig. C11 : High-voltage plateau with low-gain current preamplifier.

Fig. C12 : High-voltage plateau with high-gain current preamplifier.

Fig. C13 : Number of noise counts per second per chamber as a function of the high voltage on the chamber.

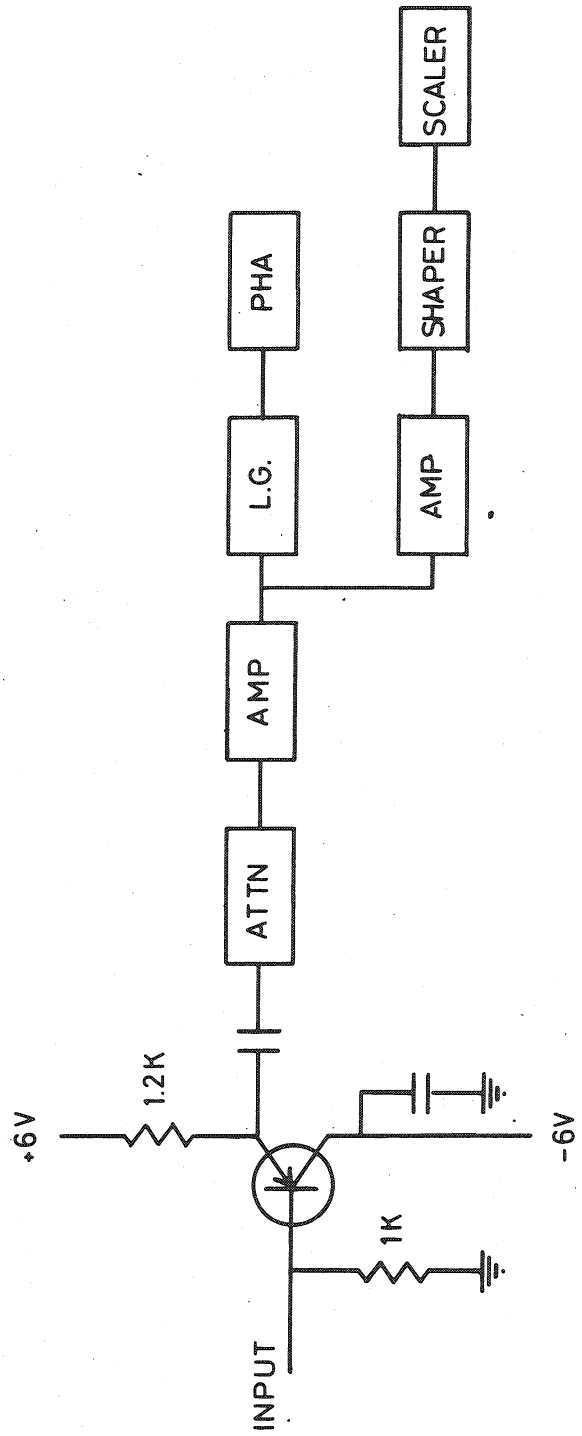

Fig. C1

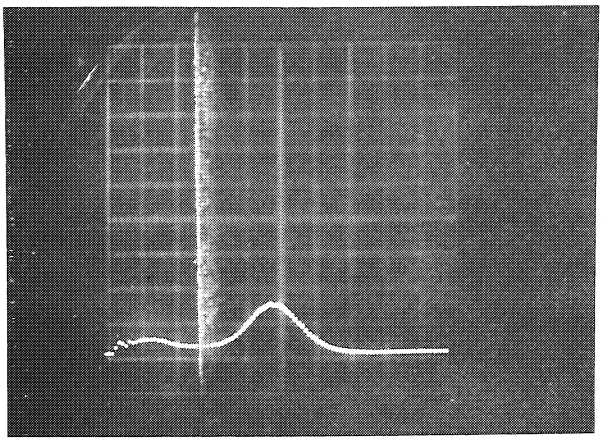

a

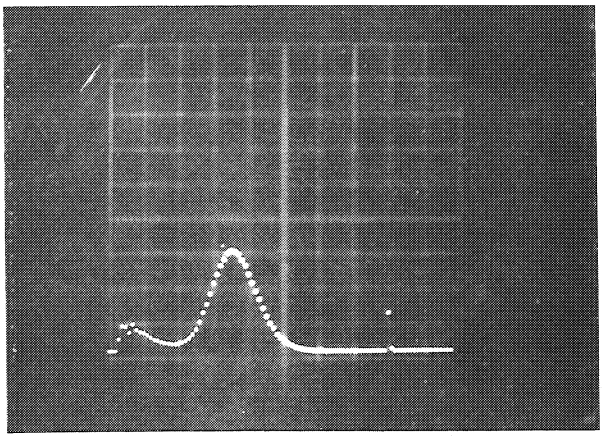

b

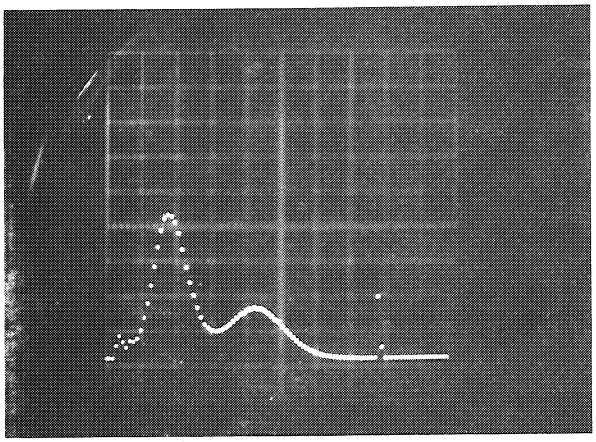

c

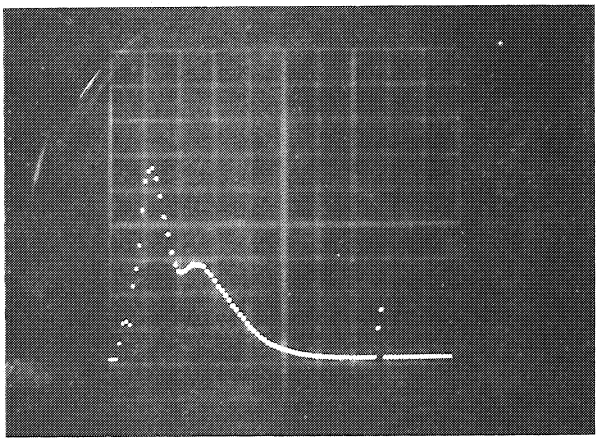

d

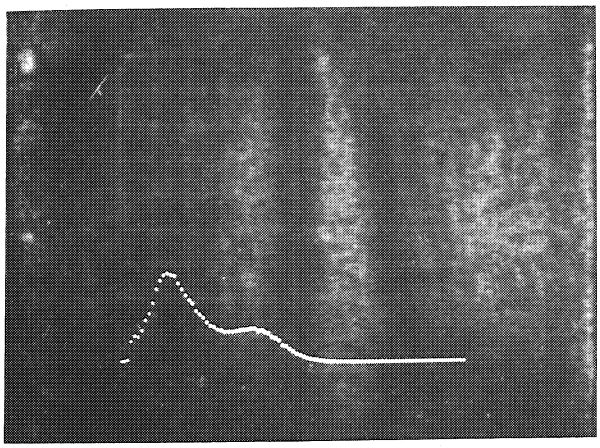

e

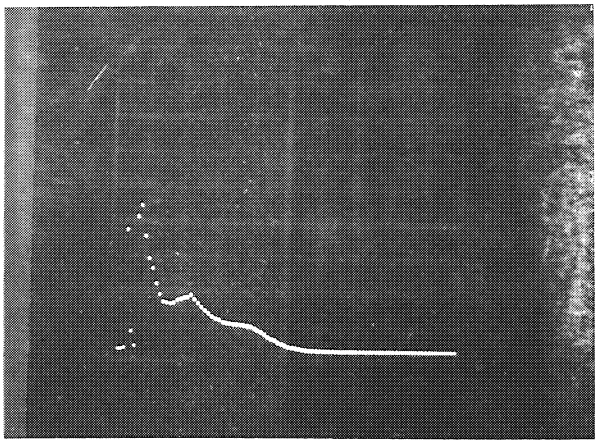

f

Fig. C2

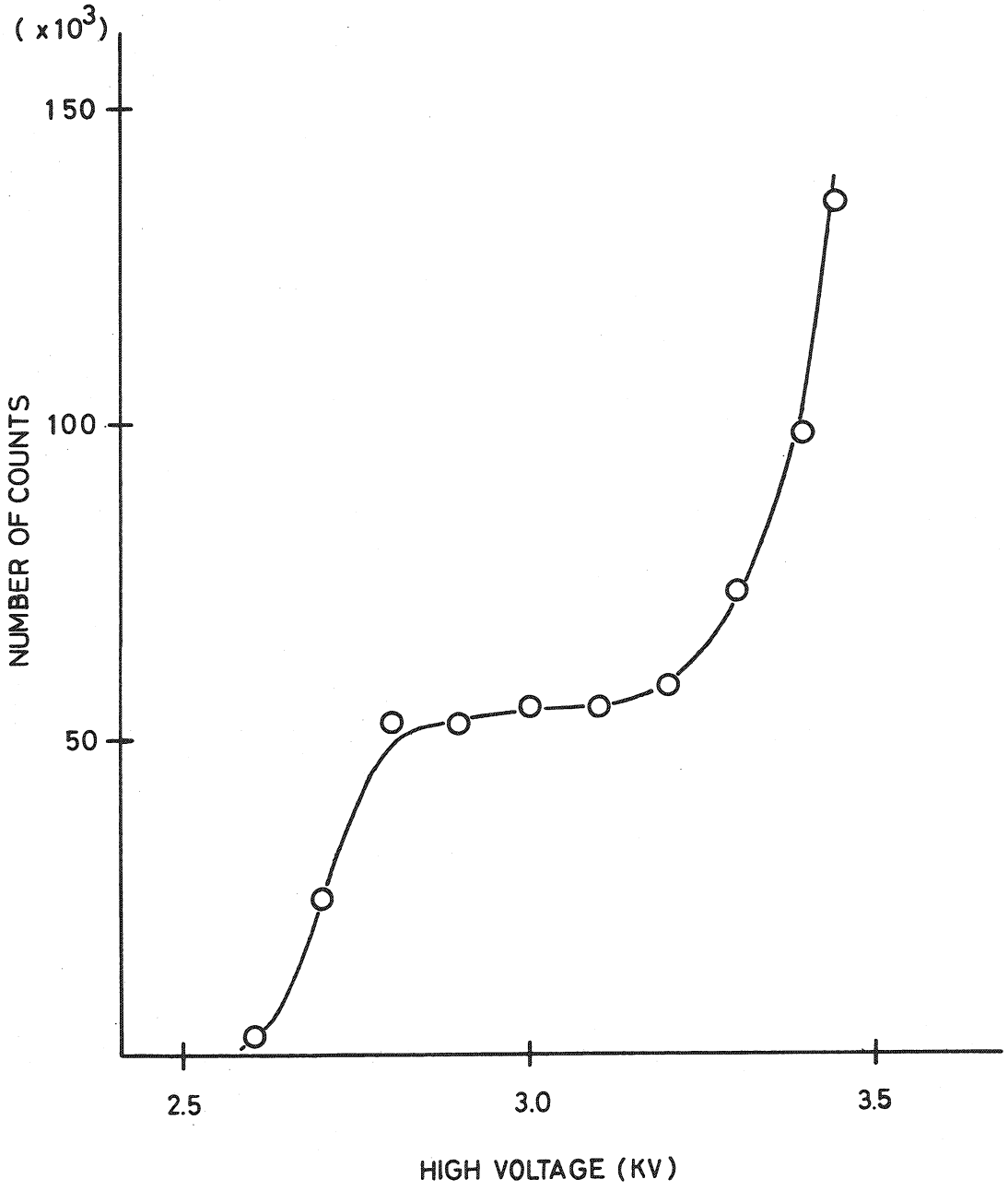

Fig. C3

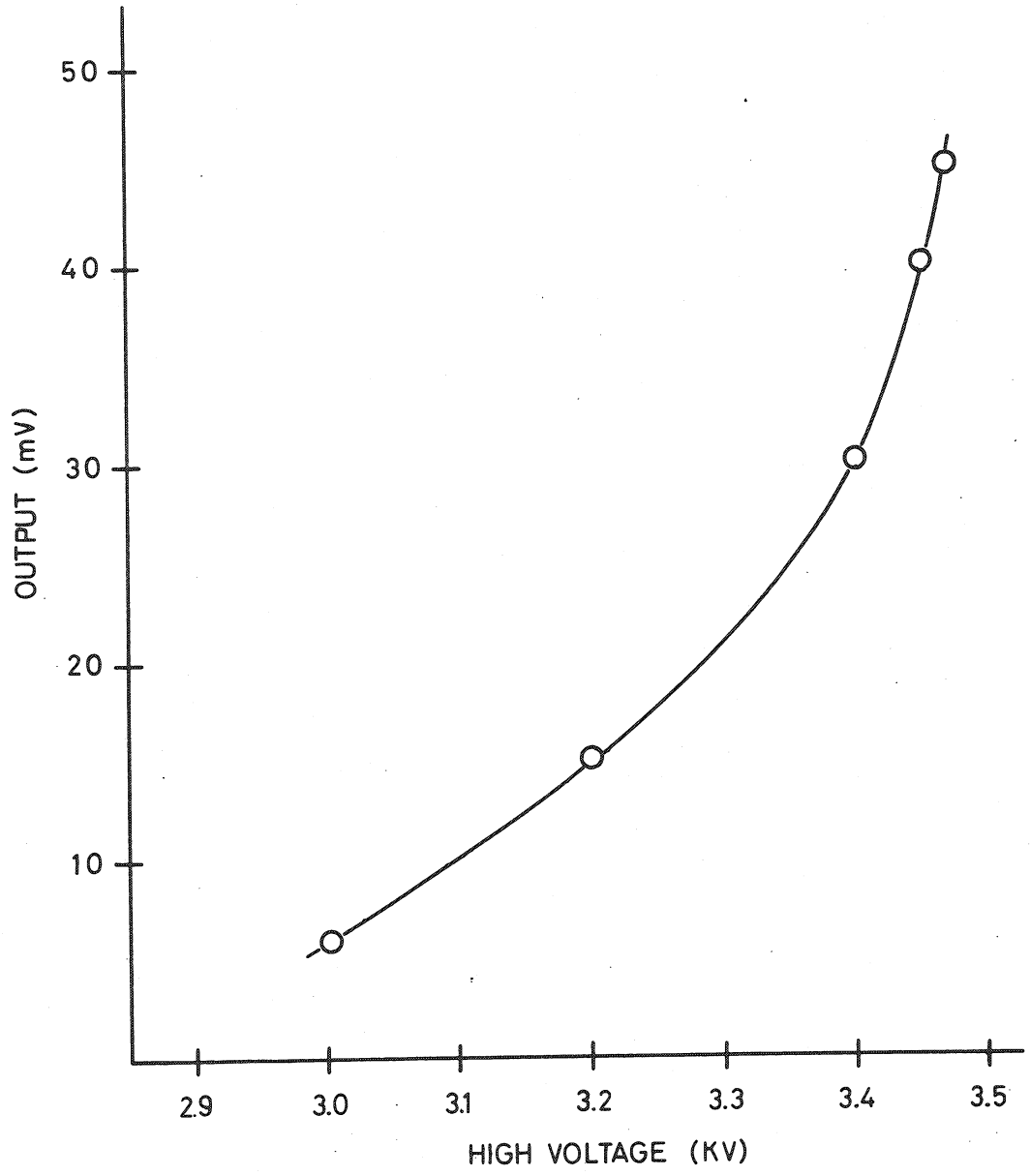

Fig. C4

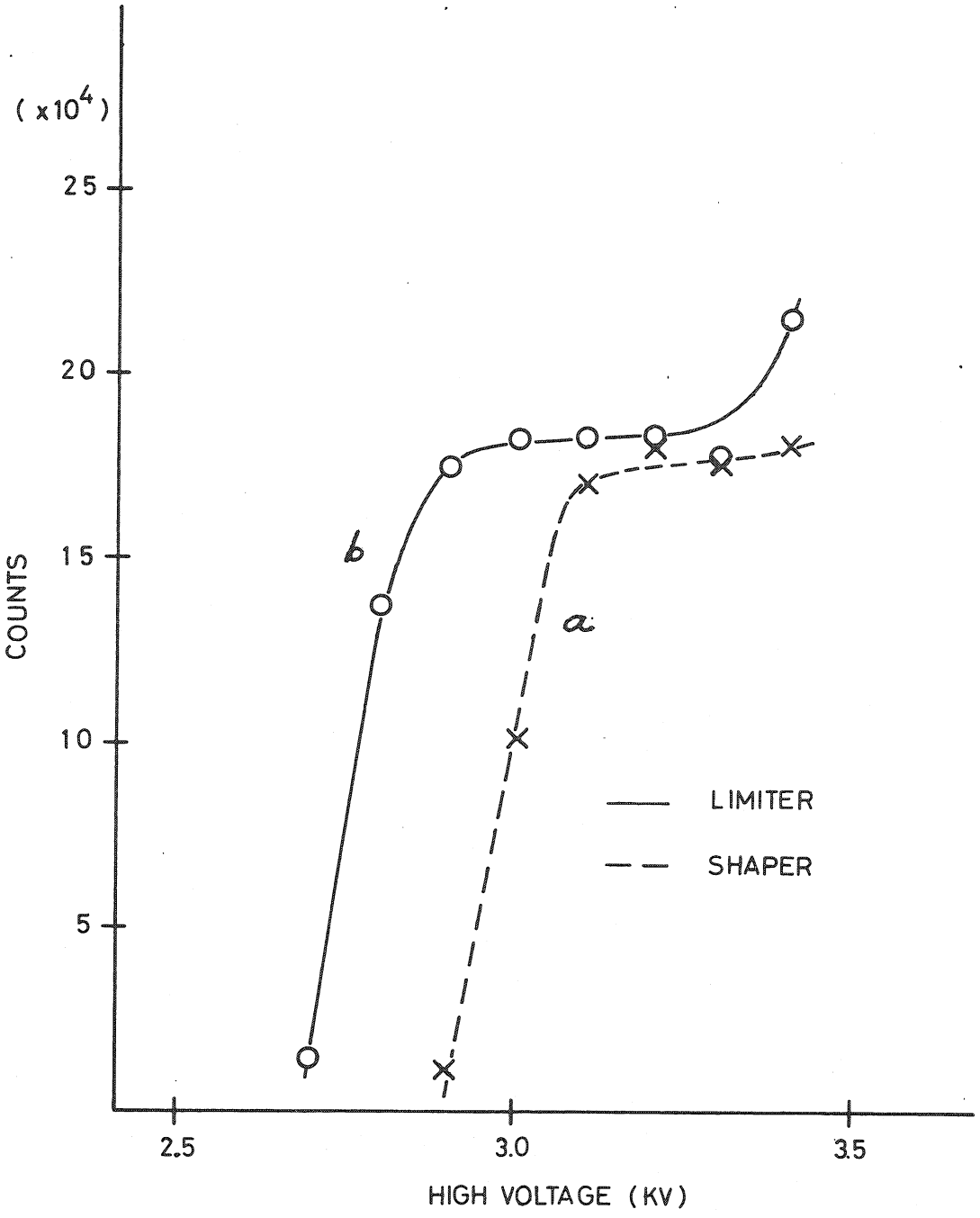
(x10^4)
25
20
15
10
5
COUNTS
b
a
LIMITER
SHAPER
2.5
3.0
3.5
HIGH VOLTAGE (KV)

Fig. C5

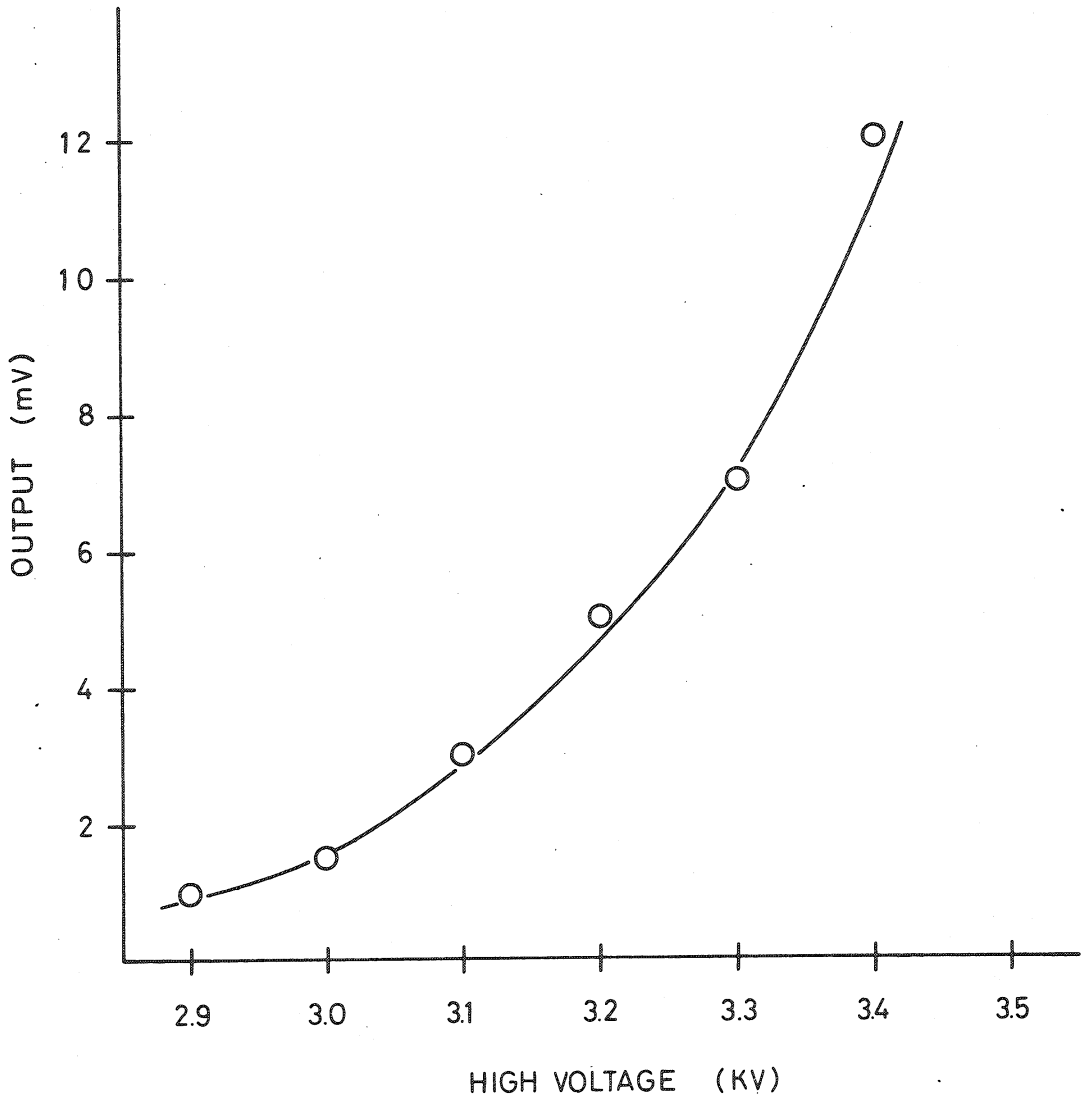

Fig. C6

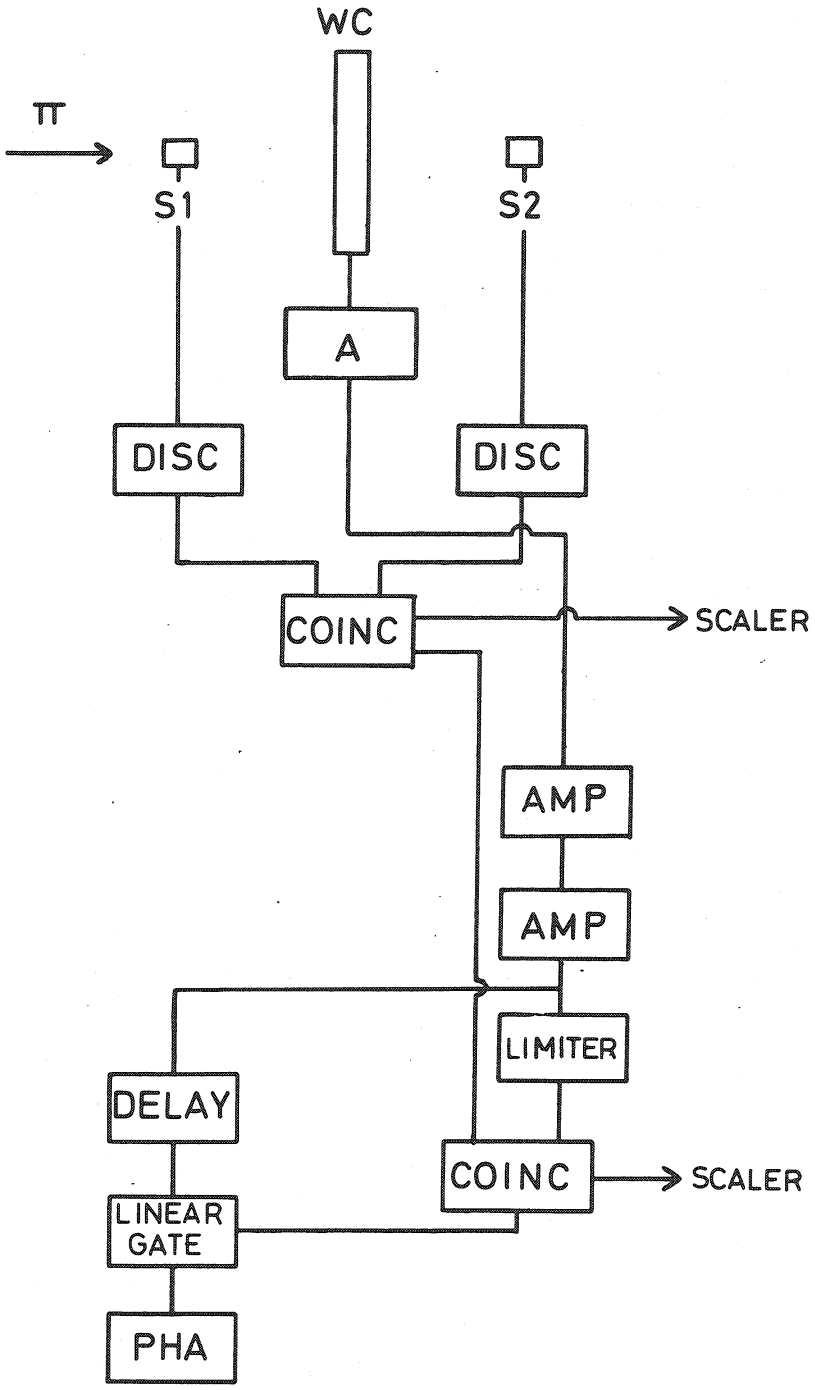
WC
π
S1
S2
A
DISC
DISC
COINC
SCALER
AMP
AMP
LIMITER
DELAY
COINC
SCALER
LINEAR GATE
PHA

Fig. C7

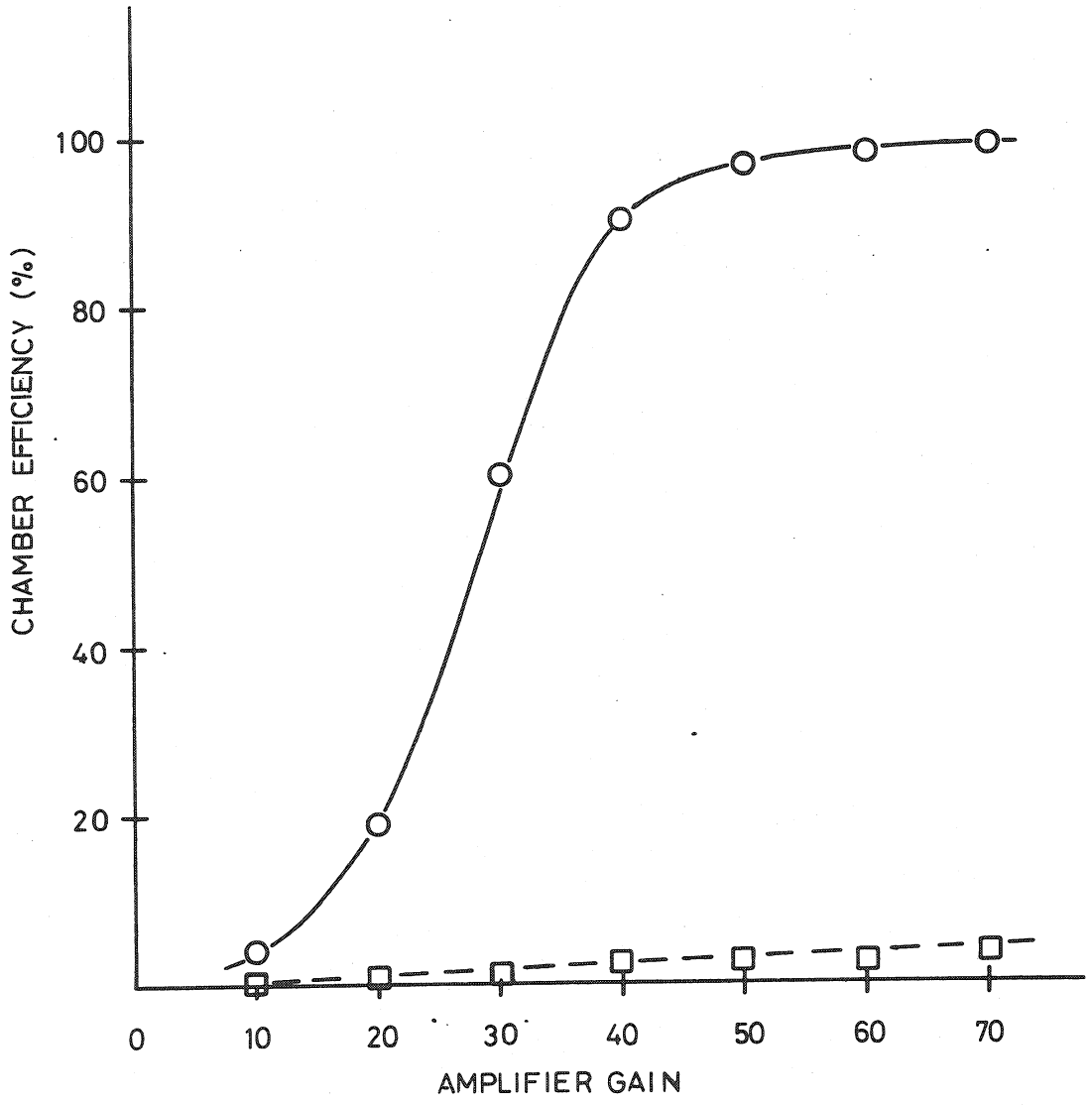
CHAMBER EFFICIENCY (%)
100
80
60
40
20
0
10
20
30
40
50
60
70
AMPLIFIER GAIN

Fig. C8

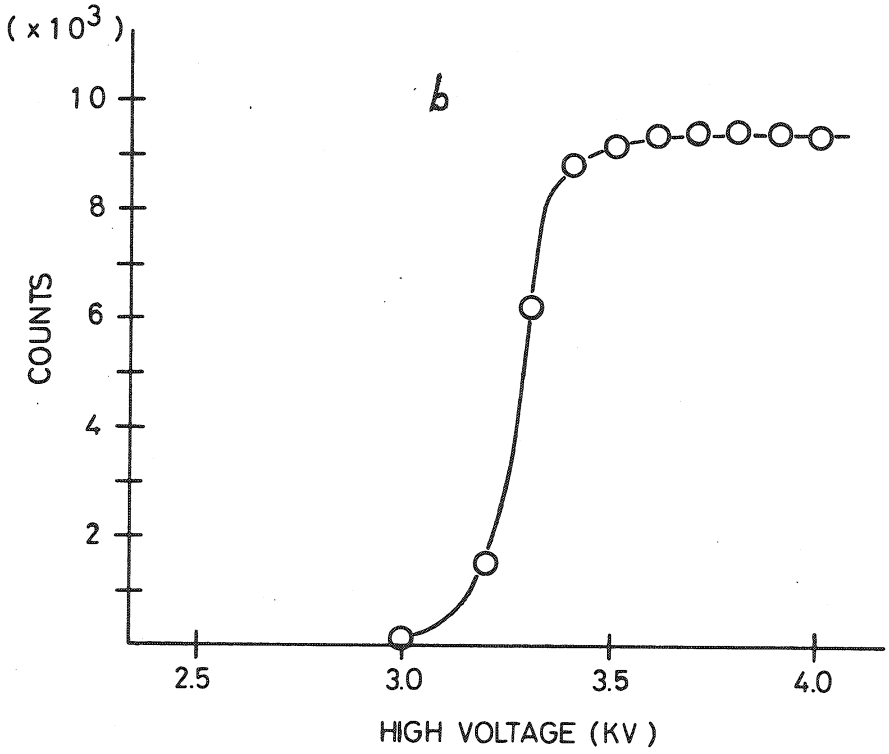
(x10³)
10
8
6
4
2
COUNTS
b
2.5
3.0
3.5
4.0
HIGH VOLTAGE (KV)

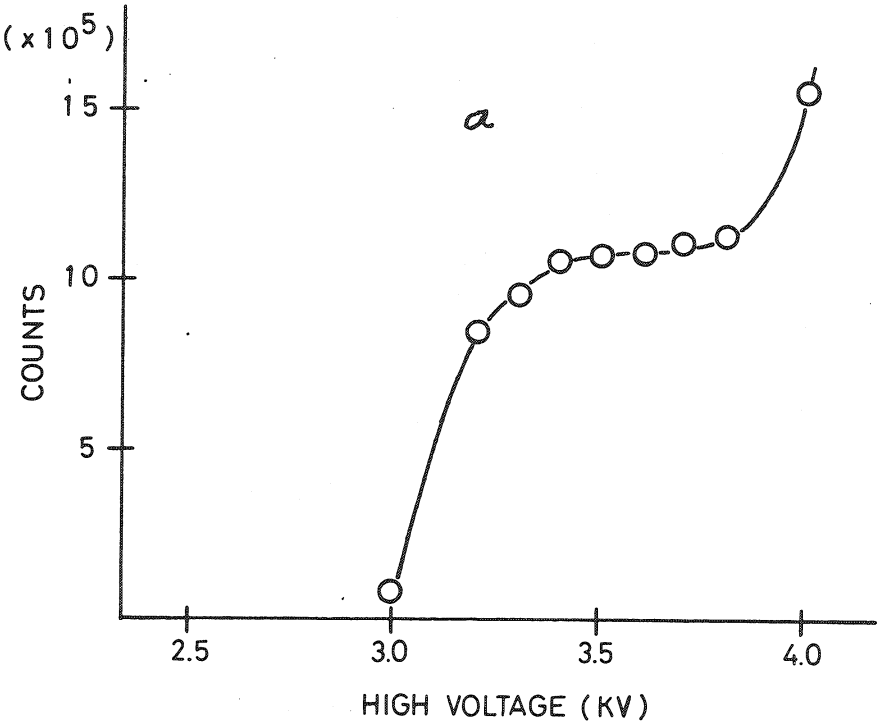
(x10⁵)
15
10
5
COUNTS
a
2.5
3.0
3.5
4.0
HIGH VOLTAGE (KV)

Fig. C9

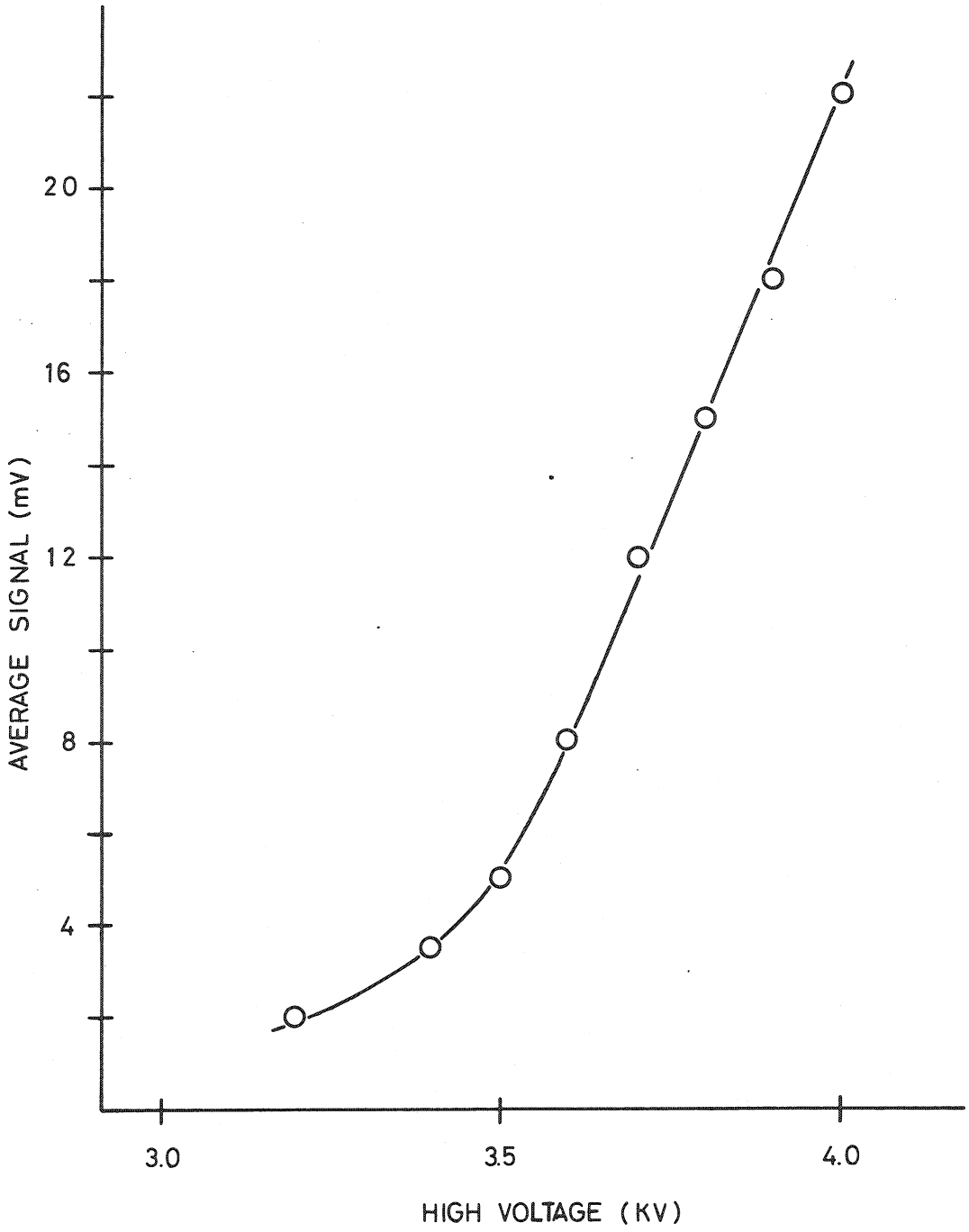

Fig. C10

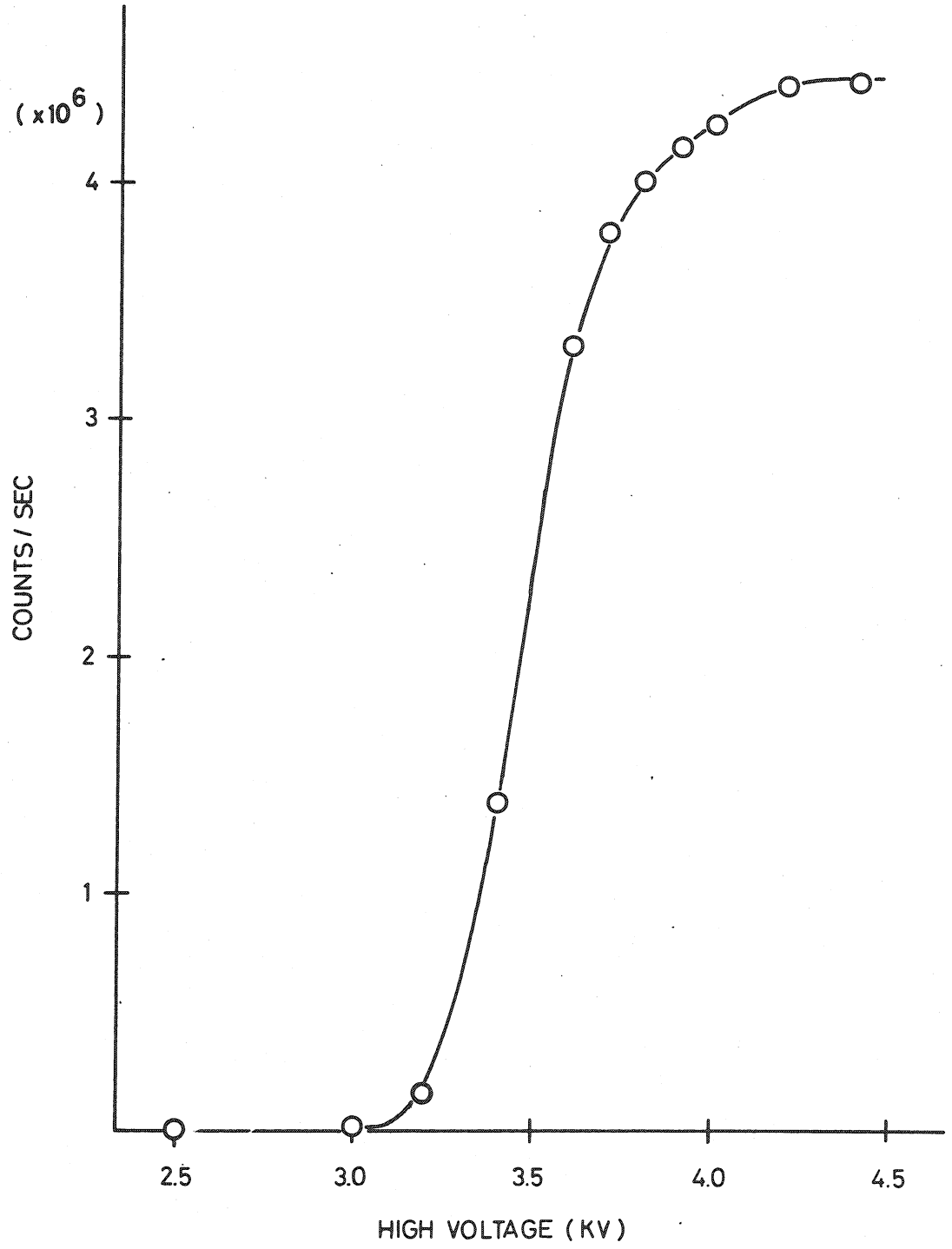

Fig. C11

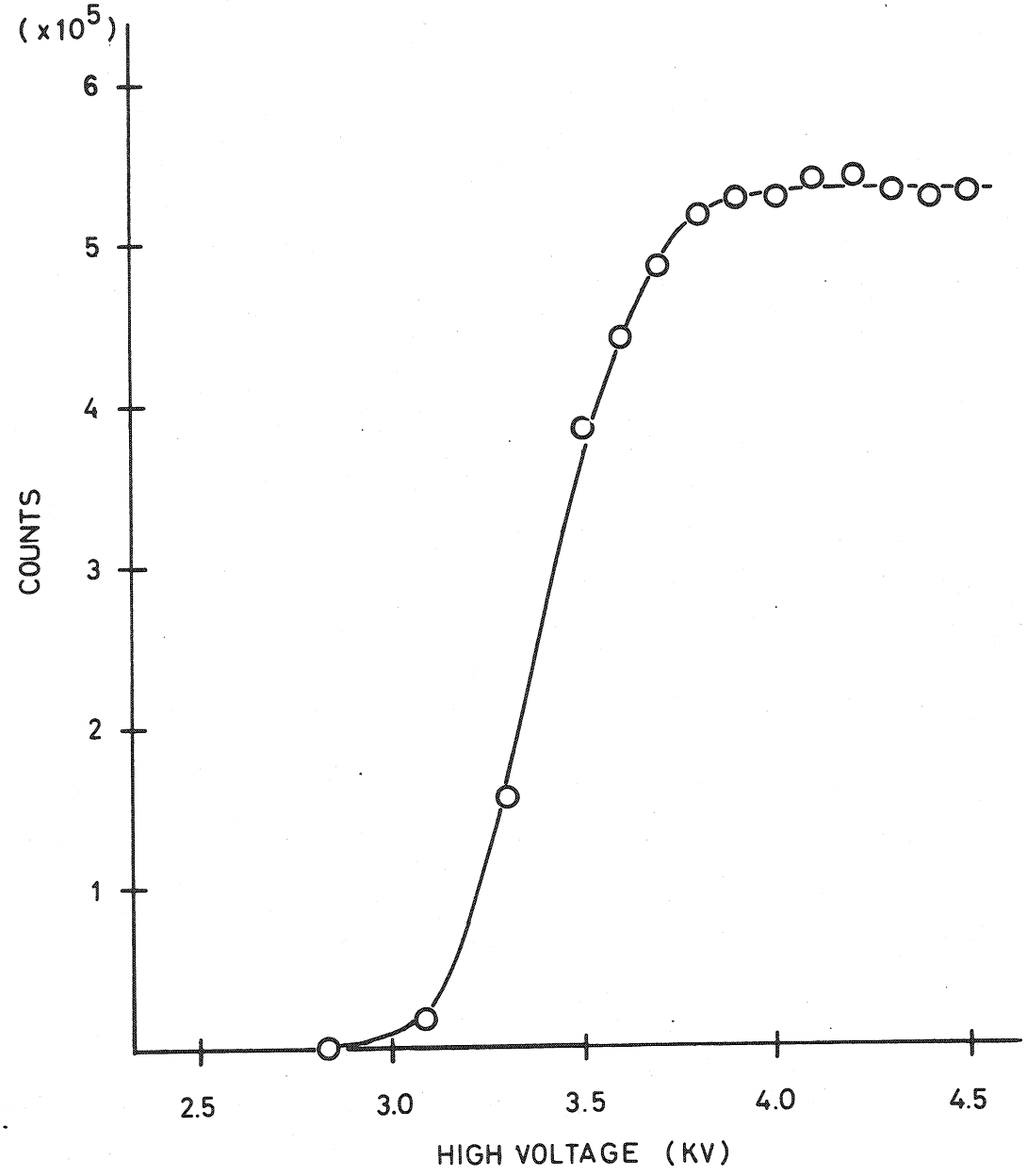

Fig. C12

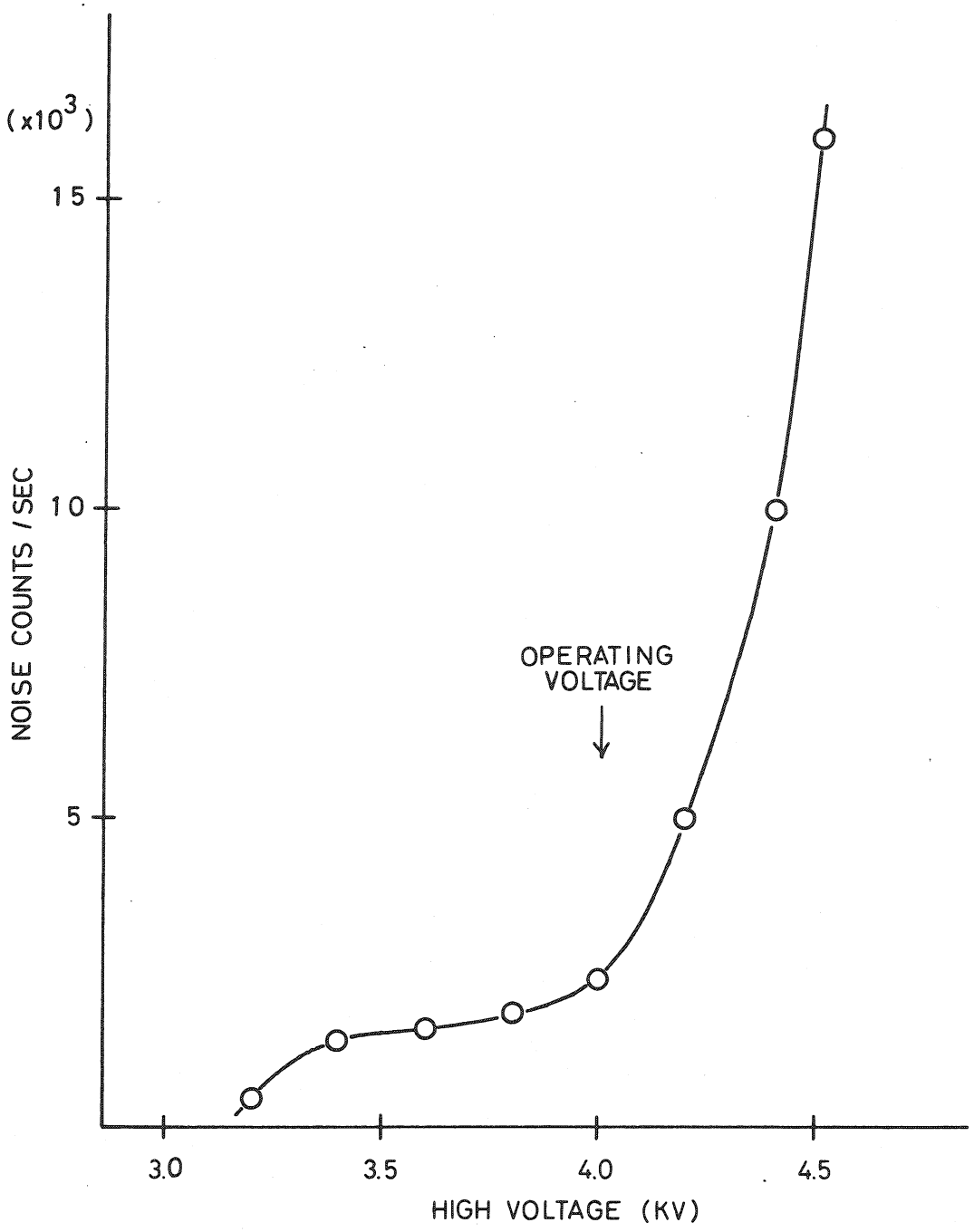
(x10^3)
15
10
5
NOISE COUNTS / SEC
OPERATING
VOLTAGE
3.0
3.5
4.0
4.5
HIGH VOLTAGE (KV)

Fig. C13